Solar Cycle Modulation of the Radiation Belt Proton Flux

ALEX J. DRAGT

Center for Theoretical Physics
Department of Physics and Astronomy
University of Maryland, College Park 20742

The purpose of this paper is to predict in an exhaustive way the solar cycle time variations to be expected in the trapped radiation belt proton flux on the assumption of a neutron decay source. By 'exhaustive' we mean that, once the interested reader decides on suitable models for the earth's atmosphere and magnetic field (we will recommend some), he should, by reading this paper, be able to predict the time variations expected for protons of any energy and pitch angle at any point in space. We have also devoted considerable attention to a derivation from the Boltzmann equation of the simplified proton transport equation commonly used in discussing energetic protons at low L values. Emphasis is given to the various approximations involved.

Despite almost 10 years of experimental and theoretical study, both the origins and time histories of radiation belt protons are quite uncertain. Shortly after the initial observations of trapped proton fluxes, it was proposed that the decay of cosmic ray albedo neutrons could serve as a satisfactory source in conjunction with atmospheric scattering as the dominant loss mechanism [*Singer*, 1958; *Lenchek and Singer*, 1962; *Hess*, 1959]. However, it is now known that there are far more protons with kinetic energies below 30 Mev than can be produced by neutron decay [*Dragt et al.*, 1966; *Vette*, 1966; *King*, 1967].

This observation has prompted re-examination of an early proposal [*Kellogg*, 1959] that the observed trapped radiation may arise from the injection of low-energy solar plasma into the earth's field at great distances followed by suitable transport and acceleration processes. The proposal appears to give correct qualitative results for protons in the energy range below 30 Mev [*Nakada et al.*, 1965; *Nakada and Mead*, 1965]. It is difficult to make detailed quantitative predictions owing to the complexity of the required calculations [*Birmingham et al.*, 1967; *Fälthammer*, 1968; *Conrath*, 1967]. Since the solar plasma is rich in α particles, a solar plasma injection source would imply that the radiation belts should also contain α particles. On the other hand, a neutron source produces an essentially pure proton belt. Alpha particles have been observed at low energies, but with somewhat less than the expected abundances [*Krimigis and Van Allen*, 1967]. There appear to be essentially no α particles at higher energies [*Fenton*, 1967].

It is difficult to invent plausible mechanisms that will effectively accelerate and transport protons having energies in excess of 30 Mev. *DeForest* [1970] extended a proposal originally made by *Birmingham* [1969] for lower energy particles to the range 40 to 110 Mev. He finds that he must invoke the presence of a worldwide fluctuating electric field having a strength of approximately 0.5 mv/m and an autocorrelation time of tens of seconds. Whether worldwide fluctuating fields exist with such short correlation times is problematical. (They should certainly be looked for. In fact, it is worth remarking that to date in studies of particles and fields, too little attention has been paid to the measurement of fields.) We do not as yet have a truly convincing mechanism of transport and acceleration that accounts for the presence of high-energy protons at low L values.

As we remarked earlier, a neutron decay source is insufficient at energies below 30 Mev. Its sufficiency at higher energies is also in question. The situation is essentially this: suppose we assume the correctness of the neutron decay hypothesis for low L values and energies above 30 Mev. Then, by using atmospheric scattering as a loss mechanism and the experimental proton data of *Freden and White* [1962] or others, it is possible to deduce both the spectrum and intensity of the neutron source above 30 Mev. (See the section on the qualitative nature of solutions.) The albedo neutron flux has not been reliably measured for energies above 30 Mev, but it is fairly well known at energies below 20 Mev [*Intriligator*, 1968; *Holt et al.*, 1966; *Haymes*, 1964]. Thus two pieces of information are known, a measured neutron flux below 20 Mev and an inferred flux above 30 Mev. At this point the problem with the neutron decay source mechanism becomes apparent, for if the measured and inferred fluxes versus energy are plotted, they do not join smoothly together. Instead, the intensity of the inferred flux is about 50 times greater than that obtained by extrapolating the measured low-energy flux [*Dragt et al.*, 1966; *Farley et al.*, 1969].

To be sure, the discrepancy may be made less spectacular by considering the uncertainties in both the measured and inferred fluxes. In particular, the atmospheric density used to compute the inferred flux is not well known experimentally. The tendency to lessen the discrepancy is further increased by the observation that, if only the relative magnitudes of the two fluxes could be adjusted, they would then have similar slopes and thus would join together very smoothly. Nevertheless, we conclude that, if neutron decay is indeed the source of high-energy protons, there must be an odd-looking discontinuity in the neutron spectrum at around 25 Mev.

In summary, there are currently two distinct proposals for the origin of energetic protons at low L values, and neither is as yet entirely satisfactory. In simplest form, one states that the high-energy protons at any given location arrive there only by being transported and accelerated from somewhere else; the other states that protons are directly injected into their observed location by a local source such as neutron decay. Our purpose in this paper is to show that these two proposals can be distinguished experimentally, and to derive the consequences of one of them. The argument is this: whatever transport and acceleration processes may be occurring owing to fluctuating electric and magnetic fields, each process must be described by a certain characteristic 'transport time.' At very low altitudes we see only protons having very short lifetimes. Consequently, by making measurements at sufficiently low altitudes, we can be sure that any protons observed have not had sufficient time to be transported from elsewhere and must have been produced by the conjectured local source mechanism in conjunction with the quantitatively well-understood loss process of atmospheric scattering. This argument is strengthened by the further observation that transport times probably increase with decreasing altitude, since, as the earth is approached, it is more difficult to produce fluctuating electric and magnetic fields of significance in comparison to the static fields. (Indeed, transport diffusion coefficients typically decrease with decreasing L [*Fälthammer*, 1968].) When combined, these two observations show that the effect of particle transport can be made negligibly small in comparison to the effect of a local injection mechanism (provided that such a mechanism indeed exists) by going to sufficiently low altitudes.

In this paper we assume a local injection source such as neutron decay and study the consequences of such a source primarily for protons mirroring deep in the atmosphere and thus having rather short lifetimes. For particles mirroring at low altitudes, we must take into account the solar cycle time variations in atmospheric density, hence our study is essentially a calculation of the time variations expected in the trapped flux over a solar cycle [*Blanchard and Hess*, 1964]. If good agreement is found between our predictions and experiment at low altitudes, the neutron decay hypothesis is strengthened. (It is not proved, of course, because what is actually being tested is whether an essentially spatially and directionally isotropic proton source with an E_{kin}^{-2} energy spectrum, such as that expected from neutron decay, can produce the observed trapped flux.) On the other hand, if disagreement prevails, albedo neutron decay must be only a small percentage of the total proton source as suggested by the factor of 50 mentioned earlier.

The Transport Equation

The proton radiation may be described by specifying a unidirectional flux $j^e(\alpha, E, L, t)$ at the geomagnetic equator. The quantity j^e is the number of protons per cm^2 sec ster Mev at the equator with a given magnetic shell value

L, equatorial pitch angle α, and energy E. Once j is known at the equator, its value at any other point may be determined from Liouville's theorem.

It is generally presumed, on more or less heuristic grounds, that in the absence of pitch angle and L diffusion the time evolution of j^e is governed by the equation

$$(\partial j^e/\partial t) = \bar{j}_n(\gamma t_n)^{-1} - v(\partial/\partial E)(j^e\ d\bar{E}/dx) - j^e\bar{P}_{in} \qquad (1)$$

Here $\bar{j}_n$ is the unidirectional neutron albedo flux averaged over a proton trajectory around the earth, and γt_n is the neutron lifetime including relativistic dilation. The quantity $d\bar{E}/dx$ gives the 'trajectory averaged' energy lost by a proton of velocity v in going a distance dx in the atmosphere, and $\bar{P}_{in}$ is an averaged rate for inelastic atmospheric interactions. The main aims of this section are to make the above definitions more precise and to obtain equation 1 as an approximation to the Boltzmann transport equation. Several assumptions and approximations are required. Thus it is also our purpose to examine the definitions, noting what refinements should be incorporated into more exact treatments. We also show that the derivation of (1) from 'first principles' is not entirely trivial.

Before proceeding further, we again comment on our neglect of pitch angle and L diffusion. First, it is certainly true that such diffusion does occur, so (1) should also contain terms of the form $(\partial/\partial\alpha)(\partial D_\alpha j^e/\partial\alpha)$ and $(\partial/\partial L)(\partial D_L j^e/\partial L)$. Here α is the pitch angle, and D_α, D_L are appropriate diffusion coefficients that are still largely unknown and are quite model dependent. (The fact that the D values are model dependent is ultimately fortunate, of course, because then we can learn from experiments.) But, although diffusion terms are present, they become unimportant at sufficiently low altitudes in comparison with the other terms provided that the conjectured source term, $\bar{j}_n$, is nonvanishing. We reason as follows: at low altitudes, the loss terms $d\bar{E}/dx$ and $\bar{P}_{in}$ are very large and j^e is very small. The product of j^e with a loss term is, according to (1), of order $\bar{j}_n$. On the other hand, diffusion contributions are of order Dj^e, and, since the D's remain finite (and even tend to vanish) at small L and j^e becomes very small, terms going as Dj^e become negligible in comparison to the other terms in (1) at sufficiently low altitudes. The only exception to this argument is pitch angle diffusion caused by multiple Coulomb scattering, since its D is proportional to atmospheric density just as $d\bar{E}/dx$ and $\bar{P}_{in}$ are and therefore increases with decreasing altitude. Thus in this case the product Dj^e does not vanish at low altitudes. The importance of this effect is discussed in Appendix B.

Phase space for a single proton is six-dimensional with coordinates $\mathbf{p}$ and $\mathbf{q}$. Taken together, all the protons in the radiation belt may be considered as members of an ensemble described by a density $C(\mathbf{p}, \mathbf{q}, t)$ in the single particle phase space. The number d^6N of protons in the volume $d^3\mathbf{p}d^3\mathbf{q}$ is given by

$$d^6N = C(\mathbf{p}, \mathbf{q}, t)\ d^3\mathbf{p}\ d^3\mathbf{q} \qquad (2)$$

The density C evolves in time according to the Boltzmann transport equation

$$\partial C/\partial t + \sum_i [\dot{q}_i(\partial C/\partial q_i) + \dot{p}_i(\partial C/\partial p_i)]$$
$$= \int d^3\mathbf{p}'C(\mathbf{p}', \mathbf{q}, t)P(\mathbf{p}' \to \mathbf{p}; \mathbf{q}, t)$$
$$- C(\mathbf{p}, \mathbf{q}, t) \int d^3\mathbf{p}'P(\mathbf{p} \to \mathbf{p}'; \mathbf{q}, t)$$
$$- C(\mathbf{p}, \mathbf{q}, t)P_a(\mathbf{p}, \mathbf{q}, t) + S(\mathbf{p}, \mathbf{q}, t) \qquad (3)$$

The left hand side of equation 3 is the total time derivative of C and would yield Liouville's theorem if the right-hand side were zero. The first term on the right says that protons of momentum $\mathbf{p}$ can result from protons of momentum $\mathbf{p}'$ interacting with the atmosphere. The probability of this happening in unit time is P. The second term says that protons are removed from momentum $\mathbf{p}$ by the same mechanism. The third term says that protons can also be completely absorbed in inelastic interactions. We discuss the exact nature of the terms P and P_a below. The last term represents protons produced by neutron decay. It is given by

$$S(\mathbf{p}, \mathbf{q}, t) = (\gamma t_n)^{-1}F(\mathbf{p}, \mathbf{q}, t) \qquad (4)$$

where F is the density of neutrons in their phase space. Here we neglect the energy of the leptons in the neutron β decay so that the proton has the same energy and direction as the parent neutron.

The 'Liouville' part of the transport equation is proved in textbooks for canonical momentums and coordinates, whereas we have written an equation involving the mechanical momentums. The canonical and mechanical momentums differ by the vector potential describing the geomagnetic field. Appendix *A* contains a proof that Liouville's theorem is also true for the mechanical momentums.

As a fast proton moves through the atmosphere, it may undergo several kinds of interactions:

I. Coulomb scattering by either free electrons, or, more predominantly, by the atomic electrons of the different atmospheric gases.

II. Coulomb scattering by the nuclei of the atmospheric gases.

III. Elastic nuclear (strong interaction) scattering by atmospheric nuclei.

IV. Inelastic nuclear interactions with atmospheric nuclei leading to the subsequent production of protons, and perhaps other particles such as neutrons, light nuclei, pions, etc.

V. Inelastic nuclear interactions without subsequent proton production or re-emission.

From the viewpoint of a transport process, the net result of interactions I through IV may be summarized by saying that there is a certain probability per unit time that a proton of momentum $\mathbf{p}'$ will disappear with the subsequent reappearance of a proton at momentum $\mathbf{p}$. For interaction I, electron Coulomb scattering, the probability per unit time is given by

$$P_{\mathrm{I}}(\mathbf{p}' \to \mathbf{p}; \mathbf{q}, t) = v'\rho_e(\mathbf{q}, t)\sigma(\mathbf{p}' \to \mathbf{p}) \qquad (5)$$

where v' is the proton speed, ρ_e is the number of electrons per unit volume, and σ is the differential Coulomb cross section for bound electrons. Strictly speaking there should be a correction for the fact that the atomic electrons are not all bound with the same energy. This effect will be shown to be negligible in a later section. The contributions from the interactions II and III are given by

$$P_{\mathrm{II,III}} = v' \sum_i \rho_i \sigma_{\mathrm{II,III}}{}^i \qquad (6)$$

Here, the quantities ρ_i are the number densities of the atmospheric constituents and the quantities $\sigma_{\mathrm{II,\,III}}{}^i$ are their nuclear Coulomb and strong elastic scattering differential cross sections, respectively.

The contribution of interaction IV is somewhat more complicated. It is possible, for example, that a fast proton may knock out one or more nucleons when colliding inelastically with an oxygen or nitrogen nucleus. A nucleus may also be left in an excited state after a collision, and this state may subsequently cool off by nucleon emission. Thus a single proton coming in may result in several protons going out. Neutrons, deutrons, tritons, and α particles may also be produced. Unfortunately the cross sections for these processes are not well known. We shall content ourselves for the moment by calling P_{IV} the net contribution of this process to transport in momentum space. It will be discussed in Appendix *B*.

By combining the effects of interactions I through IV, we find that P, the total probability per unit time for proton transport in momentum space, is given by

$$P = P_{\mathrm{I}} + P_{\mathrm{II}} + P_{\mathrm{III}} + P_{\mathrm{IV}} \qquad (7)$$

Interaction V contributes solely to proton absorption and is given by

$$P_{\mathrm{V}} = P_a = v \sum_i \rho_i \sigma_a{}^i \qquad (8)$$

where the $\sigma_a{}^i$ are total (not differential) absorption (without proton re-emission) cross sections.

To effect a solution of the transport equation as it stands would be hopelessly complicated. We will make a number of simplifying observations and approximations that will ultimately yield equation 1. We first simplify the right-hand side of the Boltzmann equation. In what follows, the notation (nt) denotes neglected terms. The effect of these terms is also treated in Appendix *B*.

We observe that P_{IV} occurs under both integral signs in equation 3. We can take into account its presence in the second integral by noting that the second integral is just the total probability (per unit time) that something besides absorption will happen to a proton of momentum $\mathbf{p}$. In particular, the integral over P_{IV} is the total probability for inelastic nuclear interaction with proton re-emission. We may thus combine the integral over P_{IV} with P_a to obtain P_{in}, the total probability (per unit time) that a proton of momentum p will undergo an inelastic nuclear interaction with or without proton re-emission,

$$P_{in} = P_a + \int P_{\mathrm{IV}}\, d^3\mathbf{p}' \qquad (9)$$

But P_{in} is a quantity that can be simply expressed in terms of known quantities. We have

$$P_{in} = v \sum_i \rho_i \sigma_{in}{}^i \tag{10}$$

where the $\sigma_{in}{}^j$ are total inelastic nuclear cross sections.

The presence of P_{IV} in the first integral cannot be dealt with in such simple fashion. We henceforth neglect its presence and will argue in Appendix B that this neglect is justifiable.

We define P_{el} to be the probability for transport due to elastic scattering,

$$P_{el} = P_{I} + P_{II} + P_{III} \tag{11}$$

The right-hand side (rhs) of (3) can then be written in the form

$$\text{rhs} = \int d^3\mathbf{p}' C(\mathbf{p}', \mathbf{q}, t) P_{el}(\mathbf{p}' \rightarrow \mathbf{p}; \mathbf{q}, t) - C(\mathbf{p}, \mathbf{q}, t) \int d^3\mathbf{p}' P_{el}(\mathbf{p} \rightarrow \mathbf{p}'; \mathbf{q}, t) - CP_{in} + S + (\text{nt}) \tag{12}$$

The function P_{el} is very strongly peaked about $\mathbf{p}' \simeq \mathbf{p}$, since both Coulomb and elastic nuclear scattering occur mostly in the forward direction. We exploit this fact by writing the first integral in equation 12 in the form

$$\int d^3\mathbf{p}' C(\mathbf{p}', \mathbf{q}, t) P_{el}(\mathbf{p}' \rightarrow \mathbf{p}; \mathbf{q}, t) = \int d^3\, \Delta\mathbf{p}\, C(\mathbf{p} - \Delta\mathbf{p}, \mathbf{q}, t) \cdot W(\mathbf{p} - \Delta\mathbf{p}, \Delta\mathbf{p}; \mathbf{q}, t) \tag{13}$$

where $\Delta\mathbf{p}$ and W are defined by

$$\Delta\mathbf{p} = \mathbf{p} - \mathbf{p}' \tag{14}$$

$$W(\mathbf{p}', \mathbf{p} - \mathbf{p}'; \mathbf{q}, t) = P_{el}(\mathbf{p}' \rightarrow \mathbf{p}; \mathbf{q}, t) \tag{15}$$

The quantity W, when viewed as a function of its second argument, is strongly peaked about $\Delta\mathbf{p} = 0$. This suggests that we expand the product CW, now viewing W as a function of only its first argument, in a Taylor series about the point $\Delta\mathbf{p} = 0$

$$C(\mathbf{p} - \Delta\mathbf{p}, \mathbf{q}, t) W(\mathbf{p} - \Delta\mathbf{p}, \Delta\mathbf{p}; \mathbf{q}, t) = C(\mathbf{p}, \mathbf{q}, t) W(\mathbf{p}, \Delta\mathbf{p}; \mathbf{q}, t) - \sum_1^3 (\partial/\partial p_i)[C(\mathbf{p}, \mathbf{q}, t) W(\mathbf{p}, \Delta\mathbf{p}; \mathbf{q}, t)] \cdot \Delta p_i + (\text{nt}) \tag{16}$$

Insertion of the expansion into the integral gives

$$\int d^3\mathbf{p}' CP_{el} = C \int d^3\, \Delta\mathbf{p}\, W(\mathbf{p}, \Delta\mathbf{p}; \mathbf{q}, t) - \sum_1^3 (\partial/\partial p_i)\left[C(\mathbf{p}, \mathbf{q}, t) \cdot \int d^3\, \Delta\mathbf{p}\, W(\mathbf{p}, \Delta\mathbf{p}; \mathbf{q}, t)\, \Delta p_i\right] + (\text{nt}) \tag{17}$$

It is easily verified that

$$\int d^3\, \Delta\mathbf{p}\, W(\mathbf{p}, \Delta\mathbf{p}; \mathbf{q}, t) = \int d^3\mathbf{p}' P_{el}(\mathbf{p} \rightarrow \mathbf{p}'; \mathbf{q}, t) \tag{18}$$

so that the first term on the right-hand side of equation 17 cancels the second term on the right-hand side of (12). To grasp the meaning of the remaining (second) term in (17) we note that $W(\mathbf{p}, \Delta\mathbf{p}; \mathbf{q}, t)$ is the probability per unit time that a proton of momentum $\mathbf{p}$ will experience a momentum transfer $\Delta\mathbf{p}$. Thus the first moment of W is just $\langle \Delta\mathbf{p}/\Delta t \rangle$, the average rate of momentum transfer due to scattering,

$$\langle \Delta\mathbf{p}/\Delta t \rangle = \int d^3\, \Delta\mathbf{p}\, W(\mathbf{p}, \Delta\mathbf{p}; \mathbf{q}, t)\, \Delta\mathbf{p} \tag{19}$$

By combining these results, we find that the right-hand side of equation 3 can be rewritten in the form

$$\text{rhs} = -\sum_i (\partial/\partial p_i)(C\langle \Delta p_i/\Delta t \rangle) - CP_{in} + S + (\text{nt}) \tag{20}$$

where the neglected terms include the earlier mentioned integral over P_{IV} and integrals over the higher order terms in the Taylor series.

A further simplification may be achieved if we assume that each proton's energy remains unchanged in the absence of scattering. This is equivalent to assuming that the electric field $\mathcal{E}$ experienced by energetic trapped protons is negligible. We let $n(E, \hat{\mathbf{\Omega}}, \mathbf{q}, t)$ denote the density of protons in 'energy and position' space, $\hat{\mathbf{\Omega}}$ denote the direction in momentum space, and E denote the relativistic energy

$$E = (m^2c^4 + p^2c^2)^{1/2} \tag{21}$$

By definition, we have

$$d^6N = nd^2\hat{\mathbf{\Omega}}\, dE\, d^3\mathbf{q} \tag{22}$$

By calculating the Jacobian, one finds

$$d^3\mathbf{p} = c^{-2}pE\, dE\, d^2\hat{\mathbf{\Omega}} \tag{23}$$

since

$$c^2p\, dp = E\, dE \tag{24}$$

Comparison of (2), (22), and (23) gives

$$n = c^{-2}pEC \tag{25}$$

We observe that the left-hand side of (3) is just the total time derivative along a particle trajectory, which we denote by D/Dt. By using this observation and energy conservation (and equation 20) we may rewrite (3) in the form

$$\begin{aligned}(Dn/Dt) &= -\sum_i pE[(\partial/\partial p_i)(\langle\Delta p_i/\Delta t\rangle np^{-1}E^{-1})] \\ &\quad - nP_{in} + c^{-2}pES + (\mathrm{nt})\end{aligned} \tag{26}$$

By symmetry, $\langle\Delta\mathbf{p}/\Delta t\rangle$ must point in the $\mathbf{p}$ direction,

$$\langle\Delta\mathbf{p}/\Delta t\rangle = (\langle\Delta\mathbf{p}/\Delta t\rangle\cdot\hat{\mathbf{p}})\hat{\mathbf{p}} \tag{27}$$

By using this fact, by observing that the sum in (26) is really a divergence that can be expressed in spherical coordinates, and by using (24) we find that

$$\sum_i pE[\ ] = c^2(\partial/\partial E)(nE^{-1}\langle\Delta\mathbf{p}/\Delta t\rangle\cdot\mathbf{p}) \tag{28}$$

Last, it is easily verified that

$$c^2E^{-1}\langle\Delta\mathbf{p}/\Delta t\rangle\cdot\mathbf{p} = \langle\Delta E/\Delta t\rangle[1 + O(\Delta p/mc)] \tag{29}$$

Thus we may also write the transport equation in the form

$$\begin{aligned}(Dn/Dt) &= -(\partial/\partial E)(n\langle\Delta E/\Delta t\rangle) \\ &\quad - nP_{in} + c^{-2}pES + (\mathrm{nt})\end{aligned} \tag{30}$$

The right-hand side of the transport equation has now been considerably simplified. We can simplify the left-hand side if we restrict our attention to protons whose lifetime T_p against atmospheric interactions is long as compared with the time they require to drift once around the earth. (For observable protons having kinetic energies greater than 30 Mev, the drift time is less than a few minutes, whereas T_p is at least several hours.) We integrate both sides of (30) along *a particle trajectory* (computed in the absence of atmospheric scattering) between the times t and $t + T$ and obtain for the left-hand side

$$\begin{aligned}\int_t^{t+T} &(Dn/Dt')\, dt' \\ &= n[\mathbf{p}(t + T), \mathbf{q}(t + T), t + T] \\ &\quad - n[\mathbf{p}(t), \mathbf{q}(t), t]\end{aligned} \tag{31}$$

If we take T to be the drift period for particles launched from the point $\mathbf{p}(t)$, $\mathbf{q}(t)$ in phase space, we have to good approximation

$$\begin{aligned}\mathbf{p}(t + T) &= \mathbf{p}(t) \\ \mathbf{q}(t + T) &= \mathbf{q}(t)\end{aligned} \tag{32}$$

since particle trajectories are very nearly periodic. (We note that (32) is correct only if the various adiabatic invariants governing a proton trajectory are conserved in the course of time. For example, if a proton encounters hydromagnetic waves, its magnetic moment may be disturbed, thus causing it to diffuse in pitch angle [*Dragt*, 1961]. Consequently in writing (32), we are tacitly neglecting field induced diffusion in pitch angle and L value.) From this observation and the assumption that n varies little in time T, we obtain

$$\int_t^{t+T} (Dn/Dt')\, dt' = T(\partial n/\partial t) + O(T/T_p)^2 \tag{33}$$

Dividing through by T converts the time integral of the right-hand side of (30) to a time average. In doing the integral, one may take n itself outside the integral sign, since it has been assumed to change little in time T. The transport equation is now brought to the form

$$\begin{aligned}(\partial n/\partial t) &= -(\partial/\partial E)(n\langle\overline{\Delta E/}\Delta t\rangle) \\ &\quad - n\bar{P}_{in} + c^{-2}pE\bar{S} + (\mathrm{nt})\end{aligned} \tag{34}$$

where the bar denotes a time average along a complete proton trajectory around the earth.

One final step is required to transform (34) into (1). We note the following relations and definitions:

$$j = vn \tag{35}$$

$$v^{-1}\langle\Delta \overline{E}/\Delta t\rangle = (d\overline{E}/dx) \tag{36}$$

$$vc^{-2}pE\bar{S} = (\gamma t_n)^{-1}\bar{j}_n \tag{37}$$

Equation 37 is the neutron counterpart of (25) and (35). The quantity $\bar{j}_n$ is the unidirectional neutron flux time averaged over a proton trajectory.

$$\bar{j}_n = T^{-1} \oint j_n[\mathbf{p}(t), \mathbf{q}(t)]\, dt \tag{38}$$

We see that all that is required to complete the transformation is to multiply (34) by v and to set $\mathbf{q}$ equal to an equatorial value.

In our discussion of this section, E has denoted the total particle energy defined in (21). In the remainder of our discussion, E will denote only the kinetic energy defined by

$$E_{\text{kin}} = (m^2c^4 + p^2c^2)^{1/2} - mc^2 \tag{39}$$

Since E and E_{kin} differ only by a constant, (1) is true for either meaning of the symbol E.

SOLUTION OF THE TRANSPORT EQUATION

In this section we transform (1) into a form amenable to numerical solution. We first discuss the detailed nature of the time averaged terms. Next we make power law fits to various quantities. Finally we make a series of algebraic substitutions to obtain a solution of the transport equation in terms of definite integrals that can be evaluated numerically.

The trajectory averaging of the albedo neutron flux was shown in a previous paper [*Dragt et al.*, 1966] with a slightly different notation. We define a globally averaged neutron escape flux j_n^{ga} by the expression

$$j_n^{ga} = (2\pi A)^{-1} \int j_n \cos\phi \, dA \, d\Omega \tag{40}$$

where the integral is taken over the surface area of the earth A and the upper hemisphere in velocity space. We next define an injection efficiency χ to be the ratio of $\bar{j}_n$ and j_n^{ga},

$$\bar{j}_n = \chi j_n^{ga} \tag{41}$$

The advantage of this definition is that it normalizes the neutron source strength to neutron fluxes measured experimentally. The quantity χ was calculated numerically for various proton orbits by using several different assumed angular distributions for j_n, and was found to be rather model independent. Typical results are given in Figures 1 through 4 of *Dragt et al.* [1966].

For the neutron flux j_n we use the model of *Lingenfelter* [1963], which has been more or less experimentally verified at neutron kinetic energies below 20 Mev. (See, for example, the references given in the introduction.) His model gives

$$j_n^{ga} = 0.04E^{-2} \text{ neutron/cm}^2 \text{ sec Mev} \tag{42}$$

We assume that this spectral shape is correct above 30 Mev, but we ignore the normalization.

The time averaging of dE/dX over proton trajectories was calculated by *Cornwall et al.* [1965] by using various models for the earth's magnetic field. To good approximation, dE/dX at any point in space is given by

$$dE/dx = -\rho_e g(E) \tag{43}$$

where ρ_e is the number of atomic electrons/cm^3 and $g(E)$ is a function of proton energy and the electron binding energy for the substance in which the electrons are bound. The dependence of g on the atomic electron binding energy is, for our purpose, not very great. For example at $E = 30$ Mev, $g = 6.8 \times 10^{-28}$ Mev cm^2 for hydrogen and $g = 5.5 \times 10^{-28}$ Mev cm^2 for air. At higher energies the discrepancy is smaller. Since most of the atmospheric interactions occur at low altitudes where the atmosphere is predominantly nitrogen and oxygen (air), and since the dependence of g on substance is relatively small, we use the g for air at all altitudes. Strictly speaking, the expression given in (43) is derived on the assumption that energy loss is due solely to electron Coulomb scattering (interaction I). However, it is experimentally known that this expression is still correct within a few per cent at energies as high as 750 Mev where nuclear interactions also play a role [*Mather and Segre*, 1951; *Barkas and Von Friesen*, 1961].

With our simplifications, the time average of dE/dx over a trajectory is given simply by

$$(d\bar{E}/dx) = -\bar{\rho}_e g(E) \tag{44}$$

Values of $\bar{\rho}_e$ for various orbits calculated in various magnetic fields are given by *Cornwall et al.* [1965]. Here it is important to realize that $\bar{\rho}_e$ varies considerably over the 11-year solar cycle, and hence j^e will also exhibit time variations.

To do the trajectory averaging for P_{in}, we note that, for the protons of interest, most inelastic interactions occur at low altitudes where the atmosphere is predominantly nitrogen or oxygen. We then have

$$\rho_{\mathrm{N}} + \rho_{\mathrm{O}} \simeq (1/7)\rho_e \tag{45}$$

by charge neutrality. Since the inelastic cross sections for nitrogen and oxygen are not very different, we obtain from (10),

$$\bar{P}_{in} = (1/7)\bar{\rho}_e v\sigma_{in}{}^N \tag{46}$$

Thus to find $\bar{P}_{in}$ we again only need $\bar{\rho}_e$. (The following section shows that only protons whose lifetime is comparable to or less than a solar cycle period display a sizeable time variation. These particles mirror at rather low altitudes; hence (45) is a good approximation over most and often all of a trajectory for protons of interest.)

We now make a series of substitutions and power law fits to prepare the transport equation for numerical work. We define a new dependent variable u by the equation

$$u(E, t) = g(E)j^e(E, t) \tag{47}$$

Then, from (1), (41), (44), (46), and (47), u obeys the equation

$$(\partial u/\partial t) = (\chi j_n{}^{ea} t_n{}^{-1})(g/\gamma) + \bar{\rho}_e(vg)(\partial u/\partial E) - (\bar{\rho}_e/7)(v\sigma_{in}{}^N)u \tag{48}$$

We make the following power law fits over the energy range 10 to 800 Mev:

$$(g/\gamma) = (8.15 \times 10^{-22})E^{-0.803} \text{ Mev cm}^2 \tag{49}$$

$$(vg) = (1.11 \times 10^{-12}) \cdot E^{-0.296} \text{ Mev cm}^3/\text{sec} \tag{50}$$

$$(v\sigma_{in}{}^N) = (1.08 \times 10^{-15})E^{0.246} \text{ cm}^3/\text{sec} \tag{51}$$

where E is measured in Mev. The fit for (g/γ) is correct to within 10%. For $g(E)$ we used the values for air given by *Rich and Madey* [1954]. The fit for (vg) is correct to within 15% over the whole energy range and is correct to within 5% below 500 Mev. The fit for $(v\sigma_{in}{}^N)$ is correct to within 15% above 50 Mev. This energy range is sufficient because nuclear interactions are unimportant below 200 Mev. The value of the cross section $\sigma_{in}{}^N$ for nitrogen has been estimated by taking the inelastic cross section for neutrons or protons on carbon and by scaling it by $(14/12)^{2/3}$ to compensate for the smaller size of the carbon nucleus. The inelastic cross section for neutrons on carbon given in *Hughes and Schwartz* [1958] was used below 100 Mev. The inelastic proton-carbon cross section (of ~200 mb) given by *Chen et al.* [1955] was used above 100 Mev.

By inserting the power law fits, we find that u obeys the equation

$$(\partial u/\partial t) = (\chi j_n{}^{ea} t_n{}^{-1})(8.15 \times 10^{-22})E^{-0.803} + \bar{\rho}_e(1.11 \times 10^{-12})E^{-0.296}(\partial u/\partial E) - \bar{\rho}_e(1.54 \times 10^{-16})E^{0.246}u \tag{52}$$

To simplify the term involving $E^{-0.296}(\partial u/\partial E)$ we introduce a new independent variable λ defined by

$$\lambda = E^{1.296} \tag{53}$$

In terms of this variable, u obeys the simpler equation

$$(\partial u/\partial t) = (\chi j_n{}^{ea} t_n{}^{-1})(8.15 \times 10^{-22})\lambda^{-0.620} + \bar{\rho}_e(1.44 \times 10^{-12})(\partial u/\partial \lambda) - \bar{\rho}_e(1.54 \times 10^{-16})\lambda^{0.19}u \tag{54}$$

We can eliminate the last term in (54) by introducing another new dependent variable G defined by the equation

$$G(\lambda, t) = u \exp[(-9.0 \times 10^{-5})\lambda^{1.19}] \tag{55}$$

It is easily verified that G obeys the still simpler equation

$$(\partial G/\partial t) = H + (1.44 \times 10^{-12})\bar{\rho}_e(\partial G/\partial \lambda) \tag{56}$$

where H denotes the 'source' term

$$H(\lambda, t) = (\chi j_n{}^{ea} t_n{}^{-1})(8.15 \times 10^{-22})\lambda^{-0.620} \cdot \exp[-(9.0 \times 10^{-5})\lambda^{1.19}] \tag{57}$$

The solution of (56), which ultimately yields the solution of (1), can be reduced to the evaluation of two definite integrals. We define a quantity $\Lambda(t')$ by the integral

$$\Lambda(t') = \lambda - (1.44 \times 10^{-12}) \int_t^{t'} \bar{\rho}_e(\nu)\, d\nu \quad (58)$$

Evidently, Λ satisfies the differential equation

$$(d\Lambda/dt') = -(1.44 \times 10^{-12})\bar{\rho}_e(t') \quad (59)$$

with the boundary condition

$$\Lambda\, |_{t'=t} = \lambda \quad (60)$$

Now we consider as a function of t' the quantity $G[\Lambda(t'), t']$. By differentiating, we have

$$\begin{aligned}(dG/dt') &= (\partial G/\partial t') + (\partial G/\partial \lambda)(d\Lambda/dt') \\ &= H[\Lambda(t'), t'] \end{aligned} \quad (61)$$

where we used equations 56 and 59. Upon integrating (61) between times t_0 and t, with the aid of (60) we obtain the result

$$G(\lambda, t) = G[\Lambda(t_0), t_0] + \int_{t_0}^{t} H[\Lambda(t'), t']\, dt' \quad (62)$$

We suppose that the t_0 is very negative. Then from (58) $\Lambda(t_0)$ becomes very positive since $\bar{\rho}_e$ is always positive. If we assume that j^e vanishes at large energies, i.e., that there is no source of infinite energy protons, then G must vanish for large positive λ. Thus, we also have the relation

$$G(\lambda, t) = \int_{-\infty}^{t} H[\Lambda(t'), t']\, dt' \quad (63)$$

By looking at (58) and (63), we see that we have achieved our announced goal of solving the transport equation in terms of definite integrals.

At this point we will comment on the net effect of the various errors we made in approximating certain quantities by power-law fits. Inspection of (48) shows that the quantity (g/γ) multiplies the neutron source term. The neutron spectral shape assumed in (42) is not known to anywhere within 10% accuracy. Thus the fitting errors made here of at most 10% are negligible compared with experimental uncertainties. The error made in fitting (vg) below 500 Mev does not exceed 5%. This is the only region where accurate comparisons with experiment can be made, since experimental flux measurements above 500 Mev are at best good to a factor of 2. Finally the presence of the term $(v\sigma_{in}{}^{N})$ numerically has only a modest effect on j^e, and a 15% error in $(v\sigma_{in}{}^{N})$ results in a considerably smaller error in j^e.

QUALITATIVE NATURE OF SOLUTIONS

In a later section we will discuss the nature of $\bar{\rho}_e(t)$ in more detail and will describe results obtained by integrating (58) and (63) numerically. In this section we analyze the solution of the transport for a time-independent atmosphere and two physically interesting limiting cases of a time-dependent atmosphere.

We suppose that $\bar{\rho}_e(t)$ is in fact a constant independent of time. Then (58) has the immediate solution

$$\Lambda(t') = \lambda - (1.44 \times 10^{-12})(t' - t)\bar{\rho}_e \quad (64)$$

We will assume that $j_n{}^{ea}$ is of the form given in (42) with some time-independent normalization coefficient A,

$$j_n{}^{ea} = AE^{-2} \quad (65)$$

Then H is time independent and is given by

$$H(\lambda) = B\lambda^{-2.16} \exp[-(9.0 \times 10^{-5})\lambda^{1.19}] \quad (66)$$

where

$$B = (\chi A t_n{}^{-1})(8.15 \times 10^{-22}) \quad (67)$$

Inserting Λ and H into (63) and changing the variable of integration gives

$$G(\lambda) = B(1.44\bar{\rho}_e \times 10^{-12})^{-1} \int_{\lambda}^{\infty} d\omega\omega^{-2.16} \cdot \exp[-(9.0 \times 10^{-5})\omega^{1.19}] \quad (68)$$

We note that G is time independent as expected. By integrating by parts, and by again changing variables of integration, we may also write

$$G(\lambda) = B(1.44\bar{\rho}_e \times 10^{-12})^{-1}(1.16\lambda^{1.16})^{-1} \cdot \exp[-(9.0 \times 10^{-5})\lambda^{1.19}][1 - K(E)] \quad (69)$$

where K is given by

$$K = z^{0.97}e^{z} \int_{z}^{\infty} \nu^{-0.97}e^{-\nu}\, d\nu \quad (70)$$

and z is related to E by

$$z = (9.0 \times 10^{-5})E^{1.54} \quad (71)$$

It is worth noting that K would vanish in the absence of nuclear interactions, is bounded between 0 and 1, and is near zero for $E < 100$ Mev.

We now undo the transformations defined in (55), (53), and (47) to get an expression for $j^e(E)$. We obtain, by using (67) and (49),

$$j^e = (\chi A t_n^{-1})(1.67\bar{\rho}_e \times 10^{-12})^{-1} \cdot E^{-0.7}\gamma^{-1}[1 - K(E)] \qquad (72)$$

This is the unidirectional flux at the equator predicted for a neutron albedo source in a time-independent atmosphere.

Figure 1 shows the actual proton omnidirectional flux at $L \simeq 1.3$ and $B/B_0 \simeq 1.41$ as measured by *Freden and White* [1962]. (Here B denotes the magnetic field strength at the point of measurement, and B_0 denotes the minimum value of B along the line $L = 1.3$.) For comparison, we also plotted the omnidirectional flux predicted at this point by the unidirectional flux j^e of (72) with the aid of Liouville's theorem. We adjusted the value of A to make theory and experiment agree at low energies. As can be

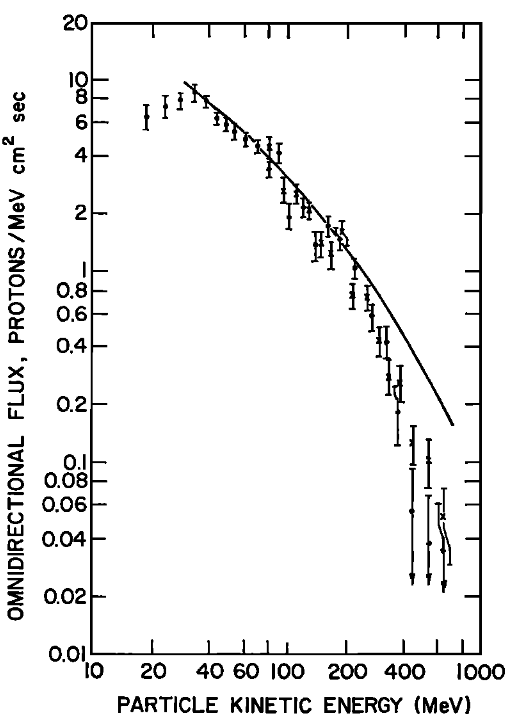

Fig. 1. Comparison of the omnidirectional flux at $L \simeq 1.3$ and $B/B_0 \simeq 1.4$ with the theoretically predicted spectral shape of Equation 72.

seen, the shape of the theoretical spectrum agrees rather well with experiment in the range 30–300 Mev. Here is the great triumph of the neutron decay theory. That is, if decaying neutrons are the primary source for these protons, the neutrons must have an energy spectrum going roughly as E^{-2} in agreement with the model of Lingenfelter given in (42). Unfortunately, as mentioned earlier, the value of A required for agreement is about 50 times larger that of (42).

If we suppose that $\bar{\rho}_e$ is time dependent, we see that two time scales enter the problem. The first is the approximately 11-year solar cycle period T_s, which governs $\bar{\rho}_e$. The second time scale is the characteristic lifetime T_p of the proton radiation against atmospheric losses. If we imagine that the neutron source leading to the j^e of (72) is suddenly turned off, then the proton flux initially decays away with a characteristic time T_p given by

$$T_p^{-1} = -(\partial/\partial t) \log j^e = (\partial/\partial t) \log G \qquad (73)$$

Use of this definition and equation 1 with no source gives

$$T_p = 6 \times 10^{11}(\bar{\rho}_e)^{-1}\tau(E) \text{ sec} \qquad (74)$$

where

$$\tau(E) = E^{1.3}(1 - K) \qquad (75)$$

The 'lifetime function' $\tau(E)$ is plotted in Figure 2.

As the reader may suspect, it is possible to obtain asymptotic solutions to the transport equation with a time-dependent $\bar{\rho}_e$ in the two extreme cases $T_p \gg T_s$ and $T_s \gg T_p$. The derivation is so tedious that we will spare details and will merely state results. We suppose, in rather good agreement with observations, that $\bar{\rho}_e(t)$ is truly a periodic function with period T_s. We may then make the Fourier expansion

$$\bar{\rho}_e(t) = \rho_0 + \sum_{n\neq 0} \alpha_n \exp(2n\pi it/T_s) \qquad (76)$$

The constant term ρ_0, which is the time average of $\bar{\rho}_e(t)$ over a solar cycle, has been explicitly separated out. We define a new dimensionless function $r(t)$ by the rule

$$r(t) = (2\pi i\rho_0)^{-1} \sum_{n\neq 0} (\alpha_n/n) \exp(2n\pi it/T_s) \qquad (77)$$

[We note that r is related to the time integral of $(\bar{\rho}_e - \rho_0)$]. Then, in the limit $T_p \gg T_s$, j^e is given by the expression

$$j^e(E, t) = j_0^e(E) \cdot [1 - r(t)(T_s/T_p) + O(T_s/T_p)^2] \qquad (78)$$

Here j_0^e is the proton flux for a time-independent atmosphere having density ρ_0 and is computed from (72) by using ρ_0 for $\bar{\rho}_e$. T_p is also evaluated by using ρ_0. We conclude that, if the proton lifetime is long compared with a solar cycle period, the proton flux shows little time variation and its magnitude is governed by ρ_0. We note that, if all frequencies higher than the fundamental are neglected, (76) through (78) state that in lowest order changes in the proton flux should lead changes in the atmosphere by 90°.

The other extreme of a short proton lifetime, $T_p \ll T_s$, can also be studied analytically. We find that, in the limit $T_p \ll T_s$, j^e is given by the expression

$$j^e = j_i^e(E, t) \cdot [1 + (7.2)MT_p\, d(\log \bar{\rho}_e)/dt + O(T_p/T_s)^2] \qquad (79)$$

Here j_i^e is the proton flux expected if the flux instantaneously inversely followed the atmosphere. It is computed from (72) by using $\bar{\rho}_e(t)$ for the electron number density. T_p is also evaluated by using $\bar{\rho}_e(t)$. M is an energy-dependent correction factor that is near 1 for low energies. Thus if the proton lifetime is short compared with a solar cycle period, the proton flux inversely follows the time variations in the atmospheric density. We also note that the first correction term has a rather large coefficient. Therefore the proton flux does not exhibit exact inverse following unless the proton lifetime is extremely short.

NUMERICAL RESULTS

In this section we describe various models for $\rho_e(t)$ and the j^e obtained from each by integrating (58) and (63) numerically. In our calculation, we used the atmospheric model of *Harris and Priester* [1962*a*, *b*]. However, we tried to present our results in such a way that they will be applicable to other atmospheric models as well.

As is well known, several solar phenomena exhibit an approximate 11-year periodicity [*Kuiper*, 1953]. One of these is the solar output

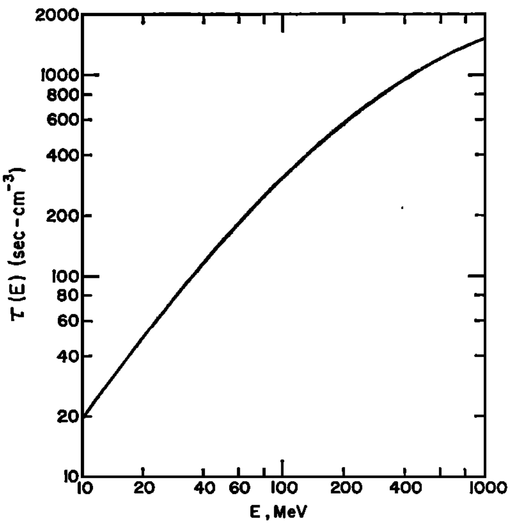

Fig. 2. 'Lifetime function.' Note that high-energy protons have a much larger lifetime than low-energy protons. As a result, high- and low-energy protons respond differently to atmospheric time variations.

of extreme ultraviolet (EUV) radiation. The EUV radiation that strikes the earth is absorbed high in the atmosphere. Consequently, fluctuations in solar EUV output produce fluctuations in the upper atmospheric temperature. Temperature fluctuations in turn produce fluctuations in the atmospheric density, since each atmospheric constituent is distributed in height h roughly according to the barometric law $\rho \propto \exp(-mgh/kT)$. It is these density fluctuations that are expected to produce fluctuations in the proton component of the radiation zone.

Because the solar EUV radiation is absorbed high in the atmosphere, it cannot be measured directly by ground-based instruments. However, it is known that solar EUV emission is closely correlated to the output of solar radio noise in the region of 2800 MHz. This is because both phenomena are related to the electron number density and temperature in the solar corona. Solar radio noise can be measured on the ground, and data have been available for several years. Time correlations between solar EUV emission, solar radio noise, and atmospheric temperature were recently examined in detail with the aid of about 3 months of satellite-measured EUV data [*Neupert*, 1965, 1967; *Bourdeau et al.*, 1964].

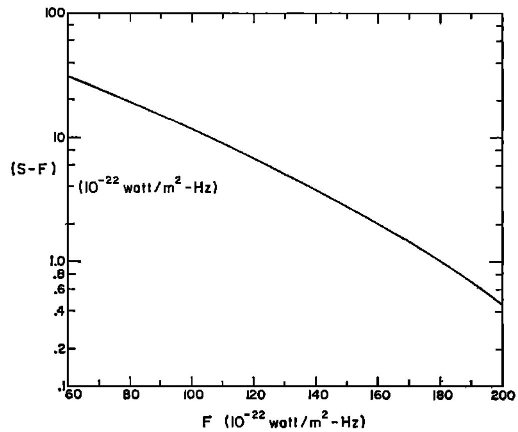

Fig. 3. Empirical relation between S and F. Here S is the model parameter of Harris and Priester, and F is the amount of solar radio noise at 2800 MHz.

Harris and Priester take into account the possible variation in EUV heating by calculating several model atmospheres. Each is labeled by a parameter S, which serves as an index of the amount of assumed EUV radiation. The quantity S was originally intended to be the amount of solar radio noise at 2800 MHz measured in units of 10^{-22} watts/m^{2}Hz. However, *Harris and Priester* [1963] found that their model gives improved agreement with actual atmospheric densities measured by using satellite drag observations if the relationship between S and the radio noise intensity (which they call F) is empirically determined. They present a graph showing the 'best' S as a function of F that is well approximated by the functional relationship

$$S = F + 31 \exp\left[-0.022(F - 60) - 0.58 \times 10^{-4}(F - 60)^2\right] \quad (80)$$

Here F is also measured in units of 10^{-22} watts/m^{2}Hz. The difference, $(S - F)$, is shown graphically in Figure 3. Quarterly averages $(\bar{F})$ of the daily values of F measured over the past several years at Ottawa [*ESSA*, 1961 through 1968] are shown in Figure 4.

As described in their paper, *Cornwall et al.* [1965] calculated $\bar{\rho}_e$ for various S values by performing orbit averages over trajectories computed in 48- and 512-term geomagnetic field models [*Jensen and Cain*, 1962; *Jensen and Whitaker*, 1960]. They also repeated their calculation with the 99-term field model of *Hendricks and Cain* [1966] (R. S. White, private communication, 1968). Their atmospheric model is the Harris-Priester atmosphere below 1000 km, and the Harris-Priester atmosphere smoothed into the *Johnson* [1962] atmosphere above 1000 km. Figures 5 and 6 show $\bar{\rho}_e$ as a function of S for particles having various minimum mirror point altitudes in the 512-term field on the field line $L = 1.4$. Results for other field lines and magnetic field models are similar. It should be noted that the averages of *Cornwall et al.* [1965] were made along the orbit of the particle's guiding center. This procedure is strictly valid only for particles with energies sufficiently small that their gyroradii are less than an atmospheric scale height [*Heckman and Brady*, 1966].

To within an error of less than 50% for most orbits of interest, $\bar{\rho}_e$ as a function of S can be fitted by the function

$$\bar{\rho}_e = a \exp\left[b(S - 100)\right] \quad (81)$$

where a and b are suitable constants. The error made in this fit is less than the uncertainties in experimental atmospheric density data. Thus, to satisfactory accuracy, each orbit for a particular magnetic field model and the Harris-Priester-Johnson atmosphere can be characterized by two parameters, a and b. We shall assume that this is always the case. That is, for any reasonable atmospheric model and magnetic field model, the resulting $\bar{\rho}_e$ will always depend on S (with S defined by equation 80) in a manner well approximated by (81) for some a and b. Values of a and b for the 48-, 99-, and 512-term fields and the Harris-Priester-Johnson atmosphere are shown in Figures 7 through 12. In summary then,

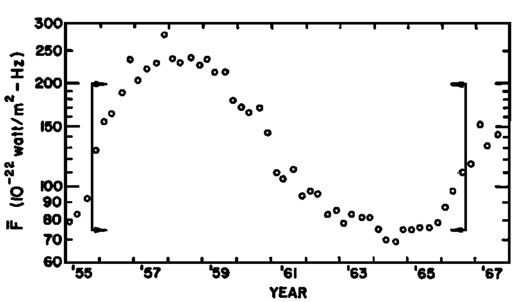

Fig. 4. Quarterly averages of the daily radio noise values at 2800 MHz. Numerical values of F are listed in Table 3. The bracketed points comprise a single solar cycle.

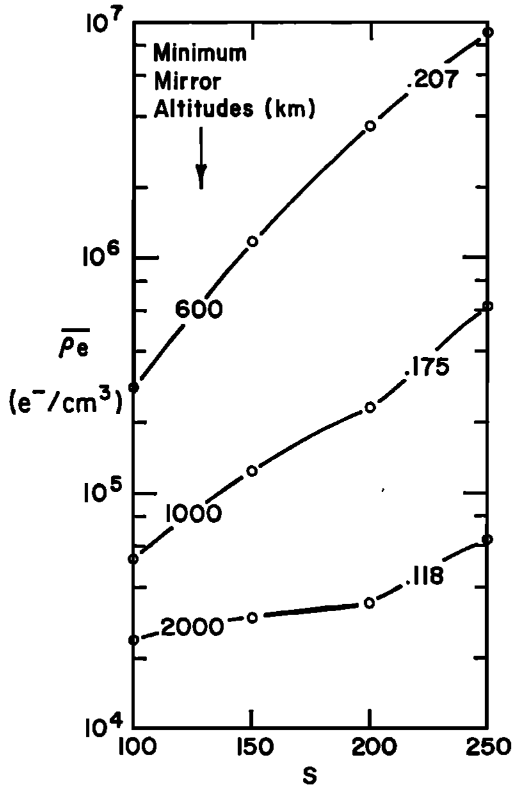

Fig. 5. Trajectory averaged electron number density $\bar{\rho}_e$ as a function of S for various orbits with $L = 1.4$. Each orbit is identified by both its minimum mirror altitude and its mirror magnetic field.

for purposes of numerical integration we take $\bar{\rho}_e(t)$ to be of the form

$$\bar{\rho}_e(t) = a \exp \{b[S(t) - 100]\} \qquad (82)$$

with $S(t)$ related to $F(t)$ by (80).

The effect of an error in $\bar{\rho}_e$ upon j^e can easily be estimated for short-lived protons that inversely follow the atmosphere. For example, if $\bar{\rho}_e$ is 50% too high, j^e will be 50% too low, etc. For longer-lived protons, the effect of a short-term change in $\bar{\rho}_e$ is less, since they tend only to be influenced by ρ_0.

The neutron albedo source j_n may also be expected to exhibit a solar cycle variation of $\sim\pm 12\%$ because of solar cycle modulation of the cosmic ray flux [*Blanchard and Hess*, 1964]. For conceptual simplicity, we took a time-independent j_n^{ga} of the form given in equation 65. The error thus made is considerably less than the error associated with uncertainties in $\bar{\rho}_e(t)$.

We also made what may be a more serious error; we assumed, in computing $\bar{\rho}_e(t)$, that a particular magnetic field model is appropriate throughout an entire solar cycle. If the geomagnetic field changes appreciably in a time comparable to a solar cycle, such changes must be taken into account. If the changes in the field are moderate, they can be accounted for by adjusting the relevant values of a and b. If the changes are immoderate, the results of this paper are invalidated. Unfortunately there are not sufficient magnetic data at present to make completely reliable statements about the field at all points within the inner radiation zone. It is known that the 48-, 99-, and 512-term field models give rather different values of $\bar{\rho}_e$ for some orbits, as evident from comparing Figures 7 through 9 [*Lindstrom and Heckman*, 1968].

What values of the model parameters are of physical interest? Figure 13 shows a, b values

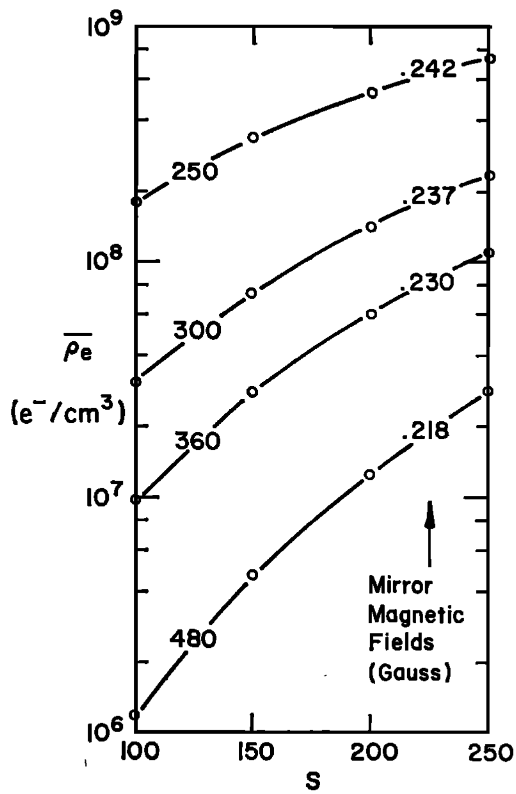

Fig. 6. Same as Figure 5.

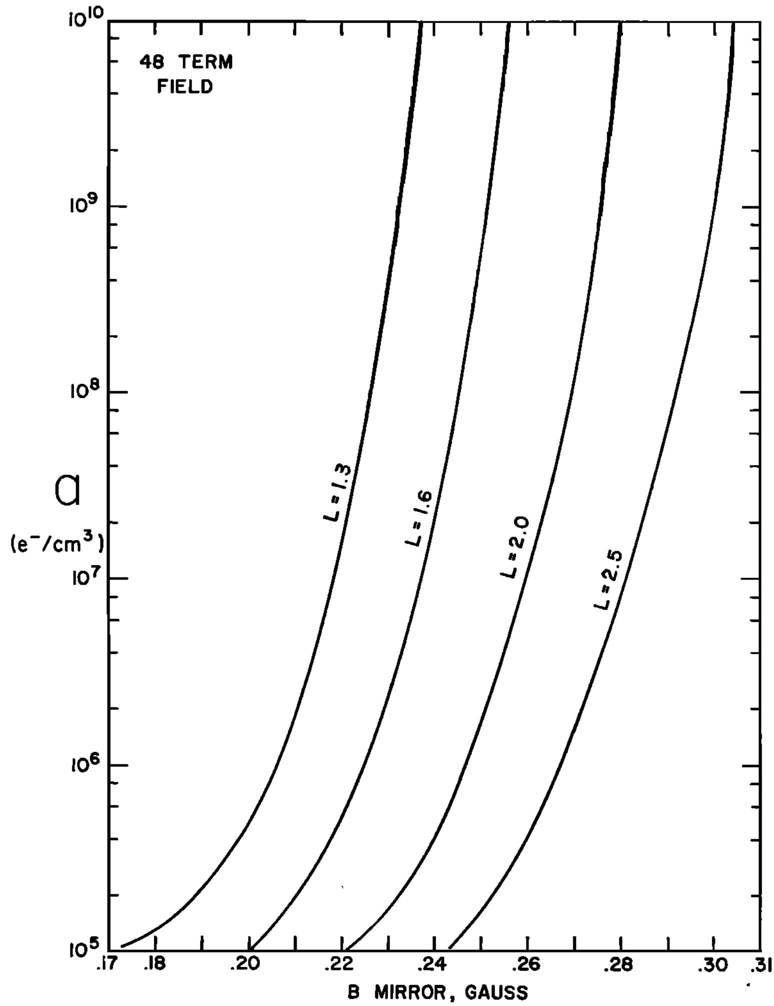

Fig. 7. 'Model parameter' a for various orbits in the 48-term magnetic field.

along the field lines $L = 1.25$ and 1.6 for the 99-term magnetic field model. Other field lines and field models give similar results. We assume that such will be the case for any physically reasonable choice of atmospheric and magnetic field models. Consequently we present only numerical results for a, b values reasonably near those in Figure 13.

We next observe that not all values of a, b require numerical integration. If b is less than 3×10^{-3}, the atmospheric density (as given by equation 81) varies less than a factor of 2 over the solar cycle. It can be proved from (58) and (63) that the variation in the proton flux can never exceed the variation in the atmosphere. Since proton flux variations of less than a factor of 2 are difficult to detect experimentally, we restrict our attention to cases where $b > 3 \times 10^{-3}$. Nor can b be too large. Values of b larger than 3×10^{-2} correspond to atmospheric density variations exceeding a factor of 90. Such variations are unrealistically large.

The values of a requiring numerical integration are restricted by somewhat different considerations. Particles in orbits for which a is small have long lifetimes. According to the previous section, the flux of such particles should exhibit little time variation. Figure 14 shows the numerically calculated time variation in flux on orbits for which $a = 10^{5}$ and $b = 0.014$. The upper curve shows $\bar{\rho}_e$ as a function of time. The average density ρ_0 is 2.8×10^6. The lower curve displays the response j^e/j_0^e for $E = 32$ Mev. Protons of higher energy show even less variation since they have a longer lifetime. Here we have used the notation of the previous section. The use of a ratio is convenient because it is independent of the absolute strength of the parent neutron flux. From (74) we find that the lifetime for the protons in question is $T_p = 6.1$ years. We see that even when the particle lifetime is comparable to a solar cycle period the proton flux still exhibits rather little time variation. Thus values of $a < 10^6$ are not of physical interest if we wish to observe time variations. The magnitude and phase of the variation are rather accurately given by the first two terms of (78). We note that the flux falls when $\bar{\rho}_e > \rho_0$, and rises when $\bar{\rho}_e < \rho_0$.

For sufficiently large values of a, we expect the proton flux to inversely follow the time variations in the atmosphere since $T_p \ll T_s$ for large a. This is indeed the case. Figure 15 shows the numerically calculated time variation when $a = 2 \times 10^7$ and $b = 0.03$ for the flux at 570 Mev. As can be seen, apart from the very-short-term atmospheric variations in 1956 and 1957, the flux nearly inversely follows the atmosphere. Also shown is the ratio j^e/j_i^e, which gives an

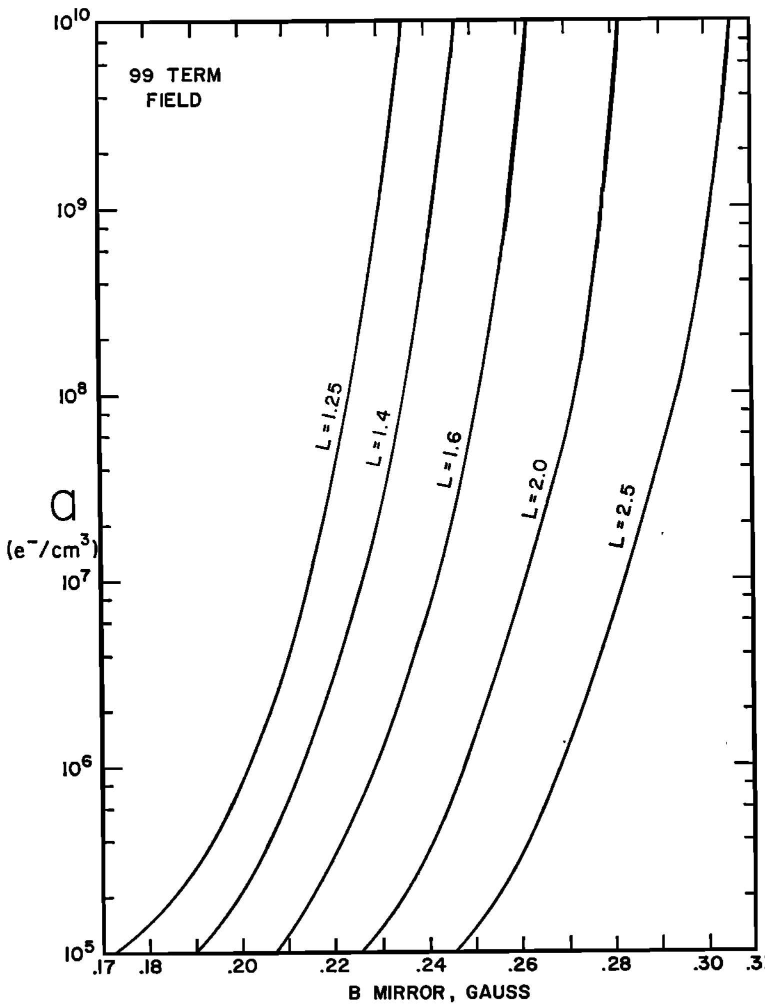

Fig. 8. 'Model parameter' a for various orbits in the 99-term magnetic field.

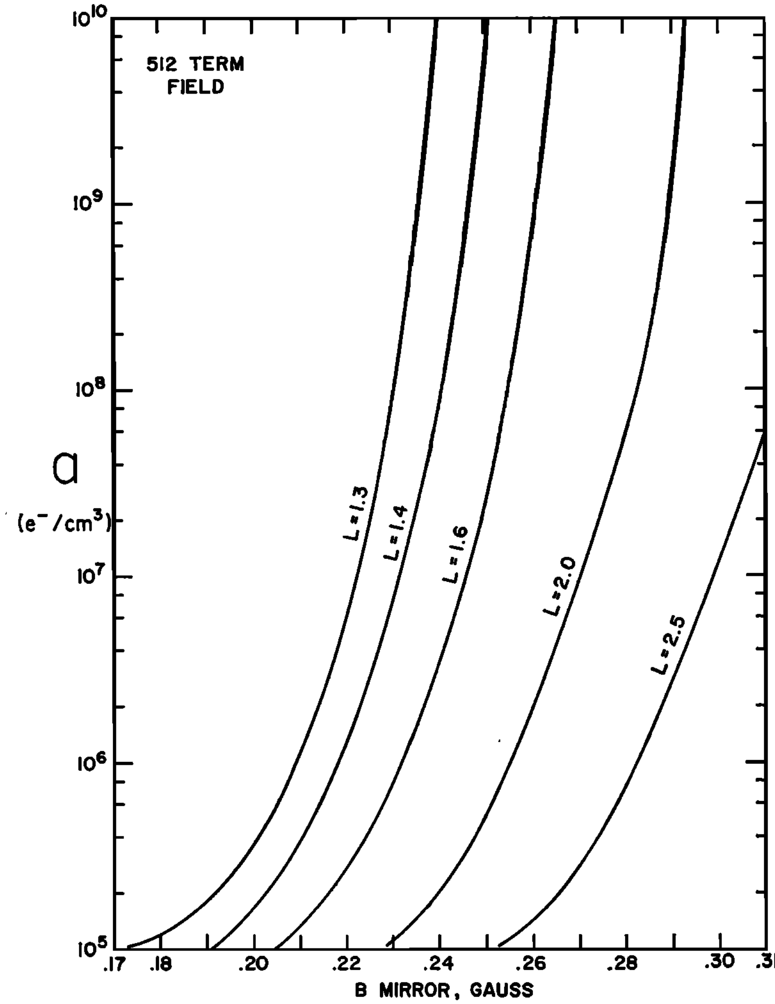

Fig. 9. 'Model parameter' a for various orbits in the 512-term magnetic field.

indication of the departure from exact inverse following. The quantity j_i^* has been computed by using a 'smoothed' ρ_e obtained by averaging out very-short-term variations. The sign and qualitative energy dependence of the departure from inverse following are given correctly by equation 79. In particular, the departure from inverse following at lower energies is considerably less, because lower energy protons have a shorter lifetime. We conclude that, to sufficient accuracy, the proton flux inversely follows the atmosphere when $a > 2 \times 10^7$.

We have seen that the proton flux shows little time variation when $a < 10^5$ and that it nearly inversely follows the atmosphere when $a > 2 \times 10^7$. This is true for all particle energies of interest. Consequently the shape of the proton energy spectrum in these two regimes should be time independent and given by equation 72. By contrast, for intermediate values of a the shape of the energy spectrum is time dependent [*Blanchard and Hess,* 1964], because, according to 75, low-energy particles have a shorter lifetime than high-energy particles. Thus the low-energy protons tend to inversely follow the atmosphere while the high-energy particles show only moderate variation. This effect is illustrated in Figures 16 and 17 for $a = 9.4 \times 10^5$ and $b = 0.024$. Figure 16 shows j^e/j_0^e as a function of time for 24- and 760-Mev protons.

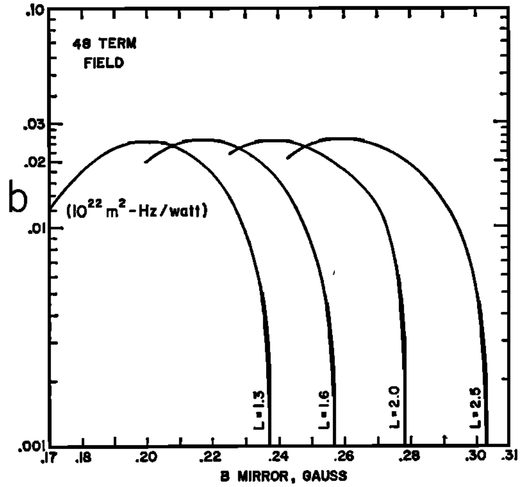

Fig. 10. 'Model parameter' b for various orbits in the 48-term magnetic field.

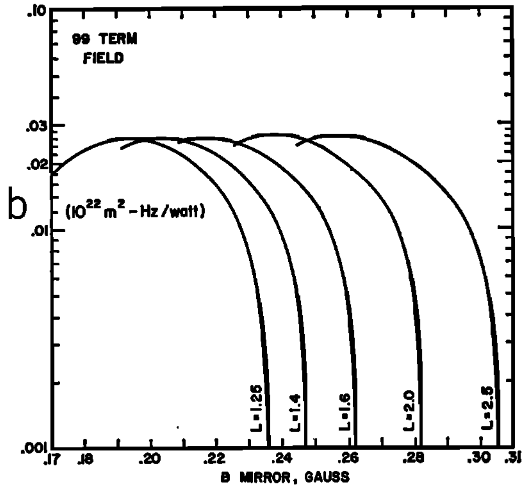

Fig. 11. 'Model parameter' b for various orbits in the 99-term magnetic field.

Figure 17 shows the energy spectrum (in arbitrary units) at two different times. The 'standard' equilibrium spectrum j_0^e is also shown. Changes in the shape of the energy spectrum may perhaps be easier to measure reliably than are time variations in the flux itself, because one need not consider the absolute calibrations of instruments flown several years apart, or make measurements at exactly the same values of B_m and L.

We end our discussion with a tabulation of numerical results and instructions for their use. Table 1 lists the function $J(E)$ defined by

$$J(E) = [1 - K(E)]/(\gamma E^{0.7}) \tag{83}$$

This function describes the standard spectral shape that would prevail in a time-independent atmosphere. The absolute intensity of the flux j_0^e expected for such an atmosphere can be found by using ρ_0 in (72). The notation $\alpha E\beta$ means $\alpha \times 10^\beta$ as is the custom with computers.

Table 2 presents a listing of the ratio $j^e(E, t)/j_0^e(E)$ as a function of energy and time for 13 of the 14 a, b values shown as squares and circles in Figure 13. (Some of the 'data' for the circles also appear graphically in Figures 14 through 17. The data for Figure 14 are not listed since they show so little time variation.) We note that most tables include more recent years than do the graphs. Results for other a, b values can be found by interpolation. To find $j^e(E, t)$ up to a normalization, one need only multiply appropriate entries in Tables 1 and 2.

To use the tables, we suppose that we wish to compute a unidirectional flux at a given point in space. We must first choose a magnetic field model. Having done so, we can compute the mirror field B_{mirror} and the L value for the particles in question. Then we proceed to Figures 7 through 12 to find the appropriate atmospheric parameters a, b. By using the a, b values thus obtained, interpolation (if necessary) within Table 2 gives $j^e(E, t)/j_0^e(E)$. As explained earlier, this quantity is readily con-

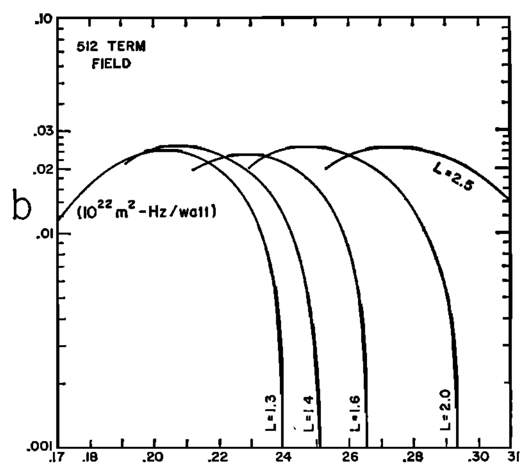

Fig. 12. 'Model parameter' b for various orbits in the 512-term field.

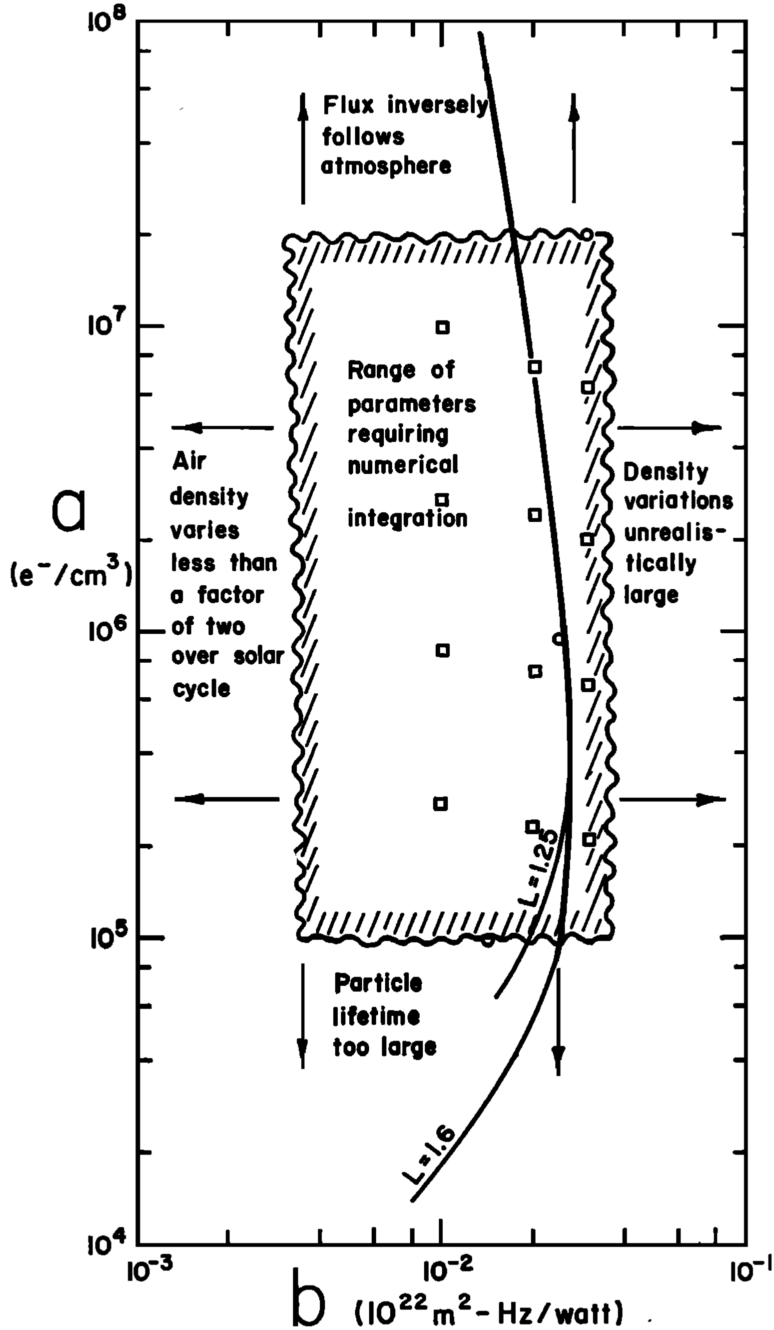

Fig. 13. Chart of 'a, b parameter space' describing various regions of interest. Squares and circles denote parameter values used in computing Table 2. The round points were also used in preparing Figures 14 through 17.

verted to $j^e(E, t)$ with the aid of Table 1 and equation 72. Finally, the desired unidirectional flux at the point of interest equals $j^e(E, t)$ by Liouville's theorem.

If the omnidirectional flux is desired, it is of course necessary to repeat the steps outlined above for several different pitch angles (values of B_{mirror}) and then to integrate over solid angle.

For convenience, Table 3 lists the values of $\bar{\rho}_e(t)$ computed for the model parameters a, b of Table 2 by using (82) and (80) and the quarterly averages $\bar{F}(t)$ shown in Figure 4. By using Tables 2 and 3 in conjunction, the interested reader can easily draw 'input' and 'response' curves as in Figure 16 to improve his physical insight and understanding. We note that the values j^e/j_0^e in Table 2 are given at midyear points in time, i.e., between the second and third quarters.

APPENDIX A. COMMENT ON LIOUVILLE'S THEOREM

We let $\mathbf{q}^c$, $\mathbf{p}^c$ and $\mathbf{q}^m$, $\mathbf{p}^m$ be, respectively, the canonical and mechanical variables describing the motion of a particle of charge Q in an electromagnetic field. They are related by the equations

$$\mathbf{q}^m = \mathbf{q}^c \qquad (A1)$$

$$\mathbf{p}^m = \mathbf{p}^c - (Q/C)\mathbf{A}(\mathbf{q}^c, t) \qquad (A2)$$

where $\mathbf{A}$ is the vector potential. We let P^c and P^m denote the number densities of ensembles of such particles in canonical and mechanical 'phase' space, respectively. If d^6N is the number of particles in a small volume element, we may write

$$d^6N = P^c\, d^3\mathbf{p}^c\, d^3\mathbf{q}^c = P^m\, d^3\mathbf{p}^m\, d^3\mathbf{q}^m \qquad (A3)$$

It is easy to compute from ($A1$) and ($A2$) that the Jacobian relating $\mathbf{q}^c$, $\mathbf{p}^c$ and $\mathbf{q}^m$, $\mathbf{p}^m$ is unity,

$$d^3\mathbf{p}^c\, d^3\mathbf{q}^c = d^3\mathbf{p}^m\, d^3\mathbf{q}^m \qquad (A4)$$

Hence, we have

$$P^c = P^m \qquad (A5)$$

More explicitly, by using ($A1$) and ($A2$), we write

$$P^m(\mathbf{q}^m; \mathbf{p}^m; t) = P^c(\mathbf{q}^c; \mathbf{p}^c; t)$$
$$= P^c[\mathbf{q}^m; \mathbf{p}^m + (Q/C)\mathbf{A}(\mathbf{q}^m, t); t] \qquad (A6)$$

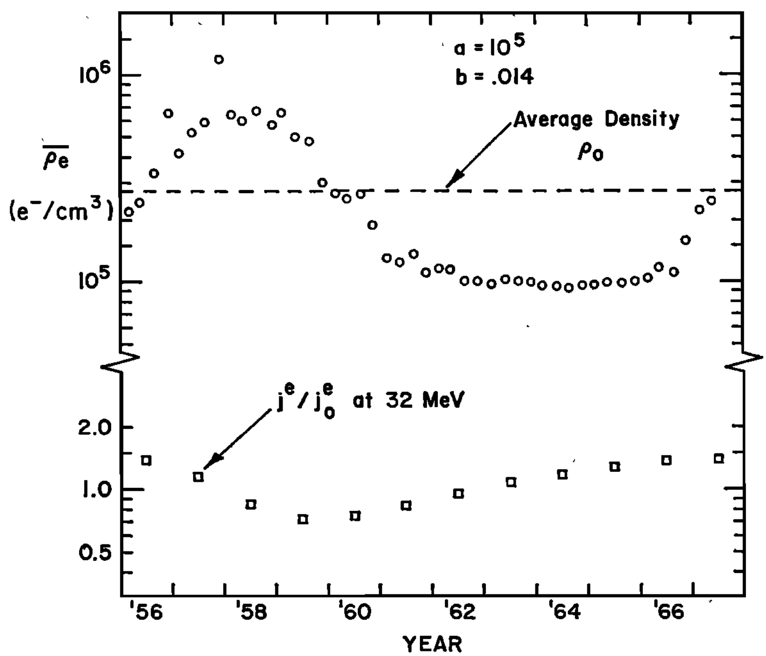

Fig. 14. The response of 'long-lifetime' 32-Mev protons to atmospheric time variations. Protons with higher energies show even less variations since they have still longer lifetimes. The unidirectional equatorial proton flux j^e is computed by using the atmospheric density $\bar{\rho}_e(t)$. The quantity j_0^e denotes the proton flux computed for a time independent atmosphere having density ρ_0.

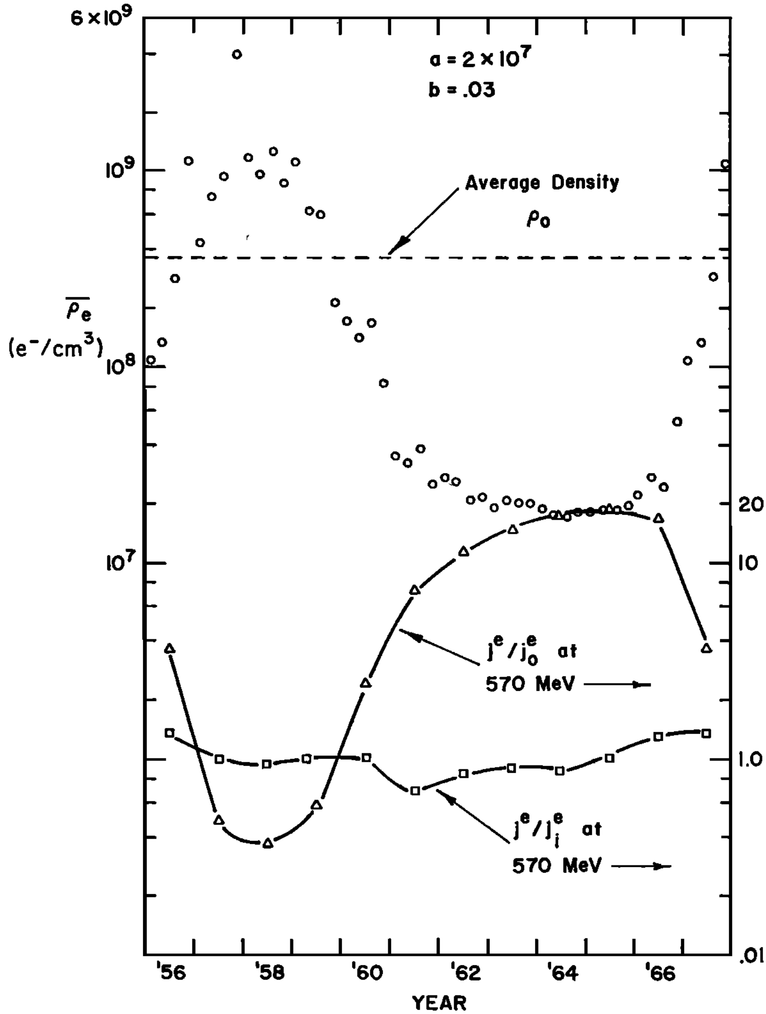

Fig. 15. The response of 'short-lifetime' protons to atmospheric time variations. The quantity j_i^e denotes the proton flux computed on the assumption that the flux inversely follows the atmosphere. We observe that the 'true' flux nearly inversely follows the atmosphere.

Now, we have the pleasure of partially differentiating with careful attention to what is being held constant and the chain rule. The quantity we wish to compute is

$$(\partial P^m/\partial t)\,|_{p^m,q^m} + \sum_i (\partial P^m/\partial q_i^m)\,|_{p^m,t}\,\dot{q}_i^m + (\partial P^m/\partial p_i^m)\,|_{q^m,t}\,\dot{p}_i^m \qquad (A7)$$

We find the following relations:

$$(\partial P^m/\partial t)\,|_{p^m,q^m} = (\partial P^c/\partial t)\,|_{p^m,q^m} = \frac{\partial P^c}{\partial t}\bigg|_{p^c,q^c} + \sum_i \frac{\partial P^c}{\partial p_i^c}\bigg|_{q^c,t}\frac{Q}{C}\frac{\partial A_i}{\partial t} \qquad (A8)$$

$$(\partial P^m/\partial q_i^m)\,|_{p^m,t} = (\partial P^c/\partial q_i^m)\,|_{p^m,t} = (\partial P^c/\partial q_i^c)\,|_{p^c,t} + \sum_j (\partial P^c/\partial p_j^c)\,|_{q^c,t}(Q/C)(\partial A_j/\partial q_i^c) \qquad (A9)$$

$$(\partial P^m/\partial p_i^m)\,|_{q^m,t} = (\partial P^c/\partial p_i^m)\,|_{q^m,t} = (\partial P^c/\partial p_i^c)\,|_{q^c,t} \qquad (A10)$$

$$\dot{q}_i^m = \dot{q}_i^c \qquad (A11)$$

$$\dot{p}_i^m = \dot{p}_i^c - (Q/C)(\partial A_i/\partial t) - (Q/C)\sum_i (\partial A_i/\partial q_i^c)\dot{q}_i^c \qquad (A12)$$

By combining all the terms and by substituting them into $(A7)$, we cancel, with the result that

$$(\partial P^m/\partial t)\,|_{p^m,q^m} + \sum_i (\partial P^m/\partial q_i^m)\,|_{p^m,t}\,\dot{q}_i^m + (\partial P^m/\partial p_i^m)\,|_{q^m,t}\,\dot{p}_i^m = (\partial P^c/\partial t)\,|_{p^c,q^c} + \sum_i \left.\frac{\partial P^c}{\partial q_i^c}\right|_{p^c,t} \dot{q}_i^c + \left.\frac{\partial P^c}{\partial p_i^c}\right|_{q^c,t} \dot{p}_i^c \qquad (A13)$$

or, as may have been obvious,

$$(DP^m/Dt) = (DP^c/Dt) \qquad (A14)$$

We conclude that Liouville's theorem applies to mechanical variables as well as to canonical variables.

APPENDIX B. DISCUSSION OF NEGLECTED TERMS

In this appendix we discuss the errors made

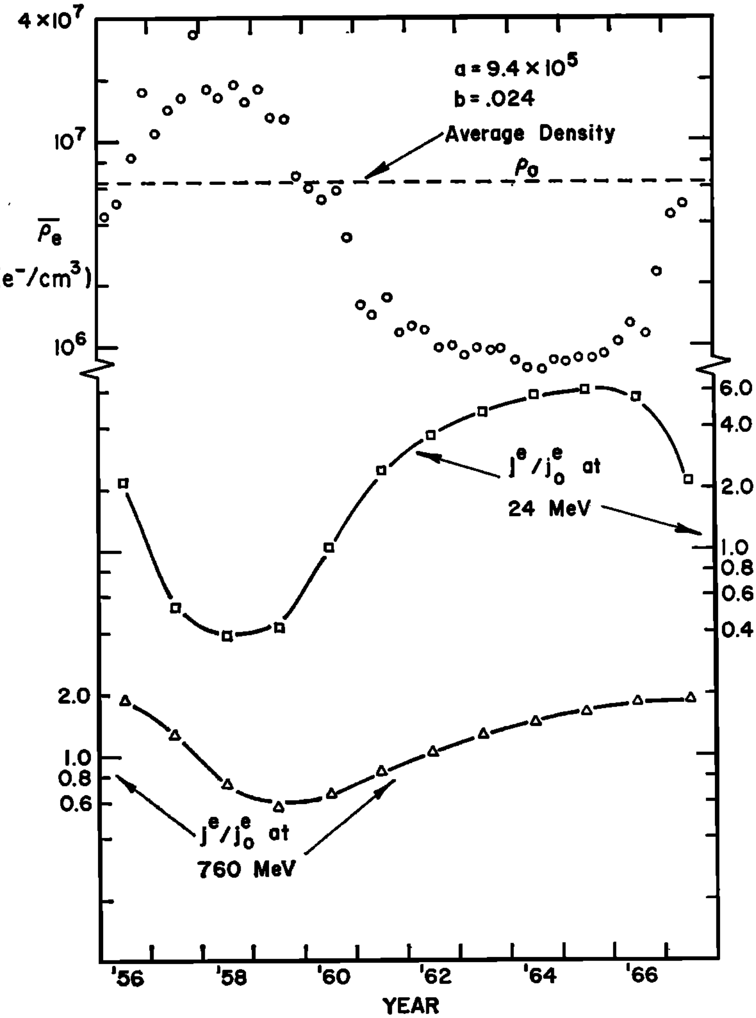

Fig. 16. The response of 'intermediate lifetime' protons to atmospheric time variations. The low-energy protons almost inversely follow the atmosphere. The high-energy protons, because of their longer lifetime, show less variation. The trajectory-averaged electron density shown in the top curve is that expected for protons having $L = 1.6$ and a minimum mirror point altitude of 510 km.

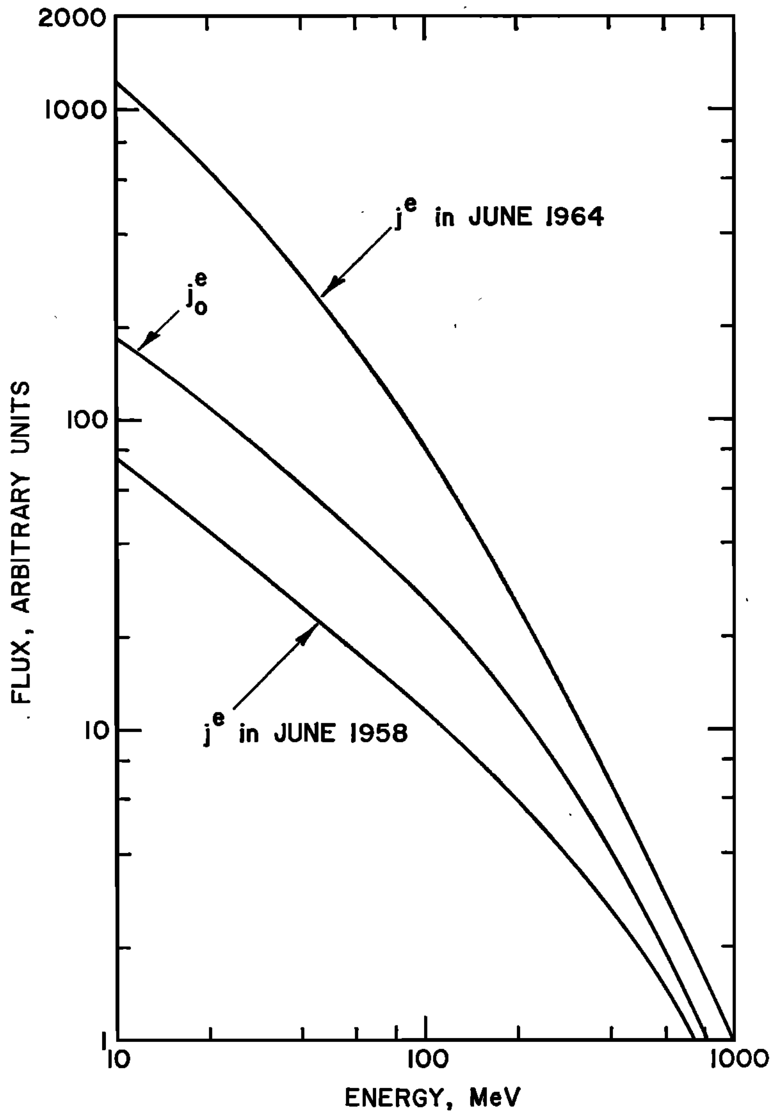

Fig. 17. Spectral shape as a function of time for the protons of Figure 16.

in neglecting P_{IV} and discarding higher order terms in the Taylor series of equation 16. We shall first treat P_{IV}. We consider the reaction

$$p + N \rightarrow N' + n \text{ protons} \qquad (B1)$$

where N is an atmospheric oxygen or nitrogen nucleus, and N' is what remains of it (including other reaction products) after a proton collision. The reaction is described in most detail by the differential cross section $d^{3n+3}\sigma/(d^3\mathbf{q}d^3\mathbf{p}_1d^3\mathbf{p}_2 \cdots d^3\mathbf{p}_n)$ where $\mathbf{q}$ is the momentum of N', and $\mathbf{p}_1 \cdots \mathbf{p}_n$ are the momentums of the outgoing protons. As may be imagined, this cross section is not well known. However, the partially integrated cross section given by

$$d^3\sigma/d^3\mathbf{p}_1 = \int [d\sigma^{3n+3}/d^3\mathbf{q}\ d^3\mathbf{p}_1 \cdots d^3\mathbf{p}_n)] \cdot d^3\mathbf{q}\ d^3\mathbf{p}_2 \cdots d^3\mathbf{p}_n \qquad (B2)$$

has been measured at various angles and energies by several authors [*Roos*, 1964; *Wall and*

TABLE 1. The Standard Spectral Shape of Equation 83

Energy, Mev	J
0.100 $E02$	0.194 E–0
0.135 $E02$	0.154 E–0
0.180 $E02$	0.122 E–0
0.240 $E02$	0.975 E–1
0.320 $E02$	0.772 E–1
0.420 $E02$	0.614 E–1
0.570 $E02$	0.468 E–1
0.760 $E02$	0.357 E–1
0.100 $E03$	0.271 E–1
0.135 $E03$	0.194 E–1
0.180 $E03$	0.136 E–1
0.240 $E03$	0.929 E–2
0.320 $E03$	0.601 E–2
0.420 $E03$	0.383 E–2
0.570 $E03$	0.216 E–2
0.760 $E03$	0.120 E–2
0.100 $E04$	0.634 E–3

Roos, 1966; *Corley*, 1968]. Fortunately, (B2) is all we need to know. We define the quantity $\sigma_{\text{prod}}(\mathbf{p} \rightarrow \mathbf{p}')$ by the rule

$$\sigma_{\text{prod}}(\mathbf{p}' \rightarrow \mathbf{p}) = d^3\sigma/d^3\mathbf{p} = (pE)^{-1}\, d^3\sigma/dE\, d\Omega \qquad (B3)$$

where $\mathbf{p}'$ is the momentum of the incident proton. The quantity P_{IV} is then given by

$$P_{\text{IV}}(\mathbf{p}' \rightarrow \mathbf{p}) = v' \textstyle\sum_i \rho_i \sigma_{\text{prod}}{}^i \qquad (B4)$$

Here, as earlier, the quantities ρ_i are number densities of atmospheric nuclei. In agreement with experiment, we again make the simplifying approximation that $\sigma_{\text{prod}}{}^i$ is the same for oxygen and nitrogen to obtain

$$P_{\text{IV}} \simeq (1/7)\rho_e v' \sigma_{\text{prod}} \qquad (B5)$$

By combining, we find that the neglected term in the transport equation is

$$\text{nt} = \rho_e (7pE)^{-1} \cdot \int d^3\mathbf{p}' C(\mathbf{p}', \mathbf{q}, t) v'\, d^3\sigma/(dE\, d\Omega) \qquad (B6)$$

Let us compare the size of this term to the source term S. By using equations 23, 25, and 35, we may also write

$$\text{nt} = \rho_e (7pE)^{-1} \cdot \int dE'\, d\Omega' j(\mathbf{p}', \mathbf{q}, t)\, d^3\sigma/dE\, d\Omega \qquad (B7)$$

We let $\sigma_0(E)$ be a number such that

$$d^3\sigma/dE\, d\Omega \leq \sigma_0(E) \qquad (B8)$$

for all $\hat{\mathbf{\Omega}}$, E', and $\hat{\mathbf{\Omega}}'$. (Of course, we must have $E' > E$.) The integral on the right hand side of (B7) can easily be estimated to give

$$\text{nt} \leq \rho_e (7pE)^{-1} \sigma_0(E) \mathcal{J}(>E) \qquad (B9)$$

where $\mathcal{J}(>E)$ is the omnidirectional flux of particles having energy greater than E. We wish

TABLE 2. The Ratio j^e/j_0^e as a Function of Time and Energy

Quantities appearing in Table 2 have the following units: a, e^-/cm^3; b, 10^{22} $m^2Hz/watt$; ρ_0, e^-/cm^3; energy, Mev.

	Energy				
	24	57	135	320	760
Time	Ratio				
$a = 2.7\ E5$	$b = 0.01$	$\rho_0 = 5.29\ E5$			
1956	1.37	1.22	1.13	1.00	1.00
1957	1.00	1.07	1.07	1.00	1.00
1958	0.74	0.90	0.95	1.00	1.00
1959	0.69	0.83	0.90	1.00	1.00
1960	0.78	0.85	0.91	1.00	1.00
1961	0.94	0.91	0.93	1.00	1.00
1962	1.10	0.98	0.97	1.00	1.00
1963	1.24	1.05	1.01	1.00	1.00
1964	1.36	1.12	1.05	1.00	1.00
1965	1.45	1.18	1.08	1.00	1.00
1966	1.49	1.23	1.11	1.00	1.00
1967	1.40	1.23	1.13	1.00	1.00
1968	1.22	1.16	1.08	1.00	1.00
1969	1.04	1.06	1.02	1.00	1.00
1970	0.92	0.98	1.00	1.00	1.00
$a = 8.7\ E5$	$b = 0.01$	$\rho_0 = 1.7\ E6$			
1956	1.38	1.41	1.28	1.16	1.11
1957	0.81	0.99	1.08	1.07	1.06
1958	0.59	0.72	0.87	0.95	0.97
1959	0.60	0.66	0.78	0.88	0.92
1960	0.83	0.77	0.81	0.88	0.91
1961	1.14	0.95	0.89	0.91	0.93
1962	1.38	1.13	0.99	0.96	0.97
1963	1.56	1.28	1.08	1.01	1.00
1964	1.69	1.41	1.17	1.06	1.03
1965	1.76	1.50	1.24	1.11	1.07
1966	1.75	1.55	1.30	1.15	1.10
1967	1.47	1.45	1.29	1.16	1.11
1968	1.18	1.24	1.20	1.12	1.08
1969	0.98	1.05	1.07	1.05	1.04
1970	0.83	0.91	0.97	0.99	1.00

TABLE 2. (*continued*)

Time	Energy 24	57	135	320	760
	Ratio				
$a = 2.7\,E6$	$b = 0.01$	$\rho_0 = 5.3\,E6$			
1956	1.22	1.39	1.46	1.40	1.31
1957	0.66	0.78	0.96	1.08	1.11
1958	0.54	0.56	0.65	0.79	0.86
1959	0.59	0.59	0.62	0.69	0.76
1960	0.92	0.83	0.76	0.75	0.78
1961	1.39	1.17	0.98	0.88	0.86
1962	1.62	1.43	1.19	1.02	0.97
1963	1.80	1.62	1.37	1.16	1.07
1964	1.91	1.75	1.51	1.28	1.16
1965	1.93	1.82	1.61	1.38	1.28
1966	1.82	1.80	1.65	1.45	1.32
1967	1.40	1.49	1.51	1.42	1.32
1968	1.12	1.19	1.26	1.26	1.22
1969	0.92	0.97	1.04	1.08	1.08
1970	0.77	0.82	0.89	0.95	0.97
$a = 1.0\,E7$	$b = 0.01$	$\rho_0 = 1.9\,E7$			
1956	1.08	1.17	1.32	1.46	1.53
1957	0.60	0.62	0.68	0.78	0.88
1958	0.53	0.53	0.52	0.53	0.55
1959	0.61	0.60	0.58	0.56	0.55
1960	0.98	0.95	0.88	0.81	0.75
1961	1.59	1.48	1.30	1.13	1.02
1962	1.75	1.70	1.58	1.41	1.28
1963	1.90	1.87	1.78	1.63	1.50
1964	2.01	1.98	1.90	1.78	1.66
1965	1.98	1.98	1.95	1.87	1.77
1966	1.80	1.84	1.88	1.86	1.81
1967	1.34	1.38	1.47	1.56	1.64
1968	1.12	1.11	1.14	1.22	1.28
1969	0.90	0.91	0.93	0.98	1.02
1970	0.75	0.76	0.79	0.82	0.85
$a = 2.3\,E5$	$b = 0.02$	$\rho_0 = 1.2\,E6$			
1956	2.55	2.02	1.47	1.23	1.14
1957	0.97	1.21	1.21	1.13	1.08
1958	0.47	0.64	0.83	0.93	0.96
1959	0.49	0.57	0.72	0.84	0.89
1960	0.83	0.72	0.77	0.85	0.89
1961	1.34	0.96	0.87	0.90	0.92
1962	1.86	1.22	0.99	0.96	0.96
1963	2.34	1.48	1.11	1.02	1.00
1964	2.75	1.72	1.23	1.08	1.04
1965	3.08	1.94	1.34	1.14	1.08
1966	3.25	2.12	1.44	1.20	1.12
1967	2.78	2.08	1.49	1.23	1.15
1968	1.98	1.75	1.39	1.20	1.13
1969	1.26	1.25	1.13	1.00	1.00
1970	0.86	0.96	0.97	1.00	1.00

TABLE 2. (*continued*)

Time	Energy 24	57	135	320	760
	Ratio				
$a = 7.4\,E5$	$b = 0.02$	$\rho_0 = 3.9\,E6$			
1956	2.46	2.67	2.26	1.75	1.50
1957	0.66	0.93	1.21	1.28	1.24
1958	0.40	0.44	0.56	0.73	0.82
1959	0.49	0.47	0.50	0.60	0.69
1960	1.08	0.85	0.71	0.69	0.73
1961	2.08	1.42	1.00	0.85	0.84
1962	2.91	2.00	1.34	1.04	0.96
1963	3.63	2.53	1.66	1.22	1.09
1964	4.13	2.97	1.95	1.40	1.21
1965	4.45	3.33	2.22	1.57	1.34
1966	4.36	3.51	2.42	1.73	1.45
1967	2.97	2.94	2.36	1.78	1.51
1968	1.88	2.05	1.91	1.60	1.41
1969	1.13	1.27	1.30	1.23	1.16
1970	0.73	0.84	0.95	0.99	1.00
$a = 2.4\,E6$	$b = 0.02$	$\rho_0 = 1.2\,E7$			
1956	1.93	2.46	2.85	2.75	2.47
1957	0.52	0.61	0.81	1.10	1.27
1958	0.39	0.38	0.38	0.41	0.47
1959	0.51	0.49	0.45	0.43	0.44
1960	1.28	1.13	0.92	0.75	0.67
1961	2.94	2.23	1.60	1.19	1.00
1962	3.80	3.12	2.30	1.67	1.36
1963	4.59	3.89	2.93	2.13	1.71
1964	5.10	4.41	3.43	2.54	2.04
1965	5.22	4.73	3.83	2.90	2.35
1966	4.67	4.59	3.99	3.15	2.60
1967	2.68	3.02	3.20	2.92	2.56
1968	1.75	1.87	2.12	2.19	2.08
1969	1.04	1.12	1.26	1.36	1.37
1970	0.64	0.70	0.80	0.90	0.95
$a = 7.4\,E6$	$b = 0.02$	$\rho_0 = 3.9\,E7$			
1956	1.60	1.86	2.35	2.89	3.15
1957	0.48	0.49	0.52	0.58	0.66
1958	0.39	0.39	0.38	0.37	0.36
1959	0.53	0.52	0.50	0.47	0.45
1960	1.37	1.32	1.22	1.08	0.97
1961	3.52	3.09	2.49	1.99	1.71
1962	4.23	3.97	3.47	2.88	2.48
1963	4.99	4.78	4.29	3.65	3.18
1964	5.55	5.29	4.83	4.22	3.74
1965	5.44	5.38	5.12	4.63	4.19
1966	4.47	4.73	4.84	4.67	4.38
1967	2.52	2.64	2.97	3.35	3.50
1968	1.77	1.73	1.78	1.99	2.19
1969	1.00	1.02	1.06	1.15	1.24
1970	0.62	0.63	0.66	0.71	0.75

TABLE 2. (*continued*)

Time	Energy 24	57	135	320	760
	Ratio				
$a = 2.1\,E5$	$b = 0.03$	$\rho_0 = 3.8\,E6$			
1956	6.13	5.00	3.16	2.06	1.66
1957	0.83	1.24	1.54	1.50	1.38
1958	0.36	0.38	0.48	0.65	0.75
1959	0.49	0.45	0.46	0.55	0.63
1960	1.48	1.01	0.74	0.68	0.71
1961	3.14	1.81	1.12	0.88	0.84
1962	4.97	2.71	1.54	1.09	0.98
1963	6.72	3.60	1.96	1.31	1.13
1964	8.22	4.44	2.37	1.53	1.27
1965	9.47	5.22	2.77	1.74	1.42
1966	10.1	5.84	3.13	1.95	1.56
1967	7.44	5.46	3.26	2.08	1.67
1968	4.26	3.93	2.77	1.93	1.59
1969	1.81	1.86	1.57	1.32	1.21
1970	0.82	0.96	1.00	1.00	1.00
$a = 6.7\,E5$	$b = 0.03$	$\rho_0 = 1.2\,E7$			
1956	5.20	6.44	5.81	4.30	3.36
1957	0.57	0.75	1.12	1.52	1.68
1958	0.37	0.35	0.33	0.34	0.30
1959	0.55	0.50	0.44	0.41	0.48
1960	2.02	1.58	1.13	0.83	0.70
1961	5.48	3.42	2.11	1.41	1.11
1962	8.49	5.45	3.23	2.04	1.55
1963	11.3	7.39	4.34	2.68	2.00
1964	13.4	9.03	5.37	3.29	2.43
1965	14.8	10.4	6.32	3.89	2.86
1966	14.2	11.0	7.05	4.42	3.26
1967	7.47	7.92	6.42	4.51	3.45
1968	3.82	4.41	4.43	3.64	2.98
1969	1.58	1.83	1.98	1.83	1.64
1970	0.66	0.79	0.94	1.02	1.03
$a = 2.0\,E6$	$b = 0.03$	$\rho_0 = 3.6\,E7$			
1956	3.71	5.21	6.79	7.02	6.43
1957	0.50	0.52	0.60	0.77	0.98
1958	0.37	0.37	0.36	0.34	0.32
1959	0.57	0.56	0.52	0.48	0.45
1960	2.33	2.11	1.75	1.39	1.17
1961	8.10	5.78	3.88	2.73	2.18
1962	11.4	8.96	6.22	4.28	3.33
1963	14.9	12.0	8.45	5.79	4.47
1964	17.2	14.2	10.3	7.18	5.55
1965	17.9	15.6	11.8	8.43	6.56
1966	15.3	14.9	12.4	9.32	7.39
1967	6.47	7.63	8.57	8.00	7.00
1968	3.63	3.80	4.48	5.00	4.96
1969	1.45	1.56	1.81	2.07	2.16
1970	0.59	0.64	0.74	0.87	0.95

TABLE 2. (*continued*)

Time	Energy 24	57	135	320	760
	Ratio				
$a = 6.4\,E6$	$b = 0.03$	$\rho_0 = 1.1\,E8$			
1956	2.91	3.40	4.54	6.16	7.26
1957	0.49	0.49	0.49	0.50	0.51
1958	0.37	0.37	0.37	0.37	0.37
1959	0.58	0.58	0.57	0.56	0.54
1960	2.45	2.40	2.27	2.07	1.90
1961	10.1	8.65	6.63	5.02	4.19
1962	13.1	12.1	10.2	8.13	6.81
1963	16.7	15.7	13.5	11.0	9.31
1964	19.5	18.1	15.9	13.3	11.4
1965	19.0	18.6	17.2	15.0	13.1
1966	14.5	15.6	16.1	15.1	13.9
1967	6.00	6.28	7.26	8.68	9.42
1968	3.74	3.57	3.50	3.85	4.36
1969	1.41	1.42	1.46	1.55	1.67
1970	0.57	0.57	0.60	0.64	0.67
$a = 2.0\,E7$	$b = 0.03$	$\rho_0 = 3.6\,E8$			
1956	2.71	2.77	2.91	3.26	3.7
1957	0.48	0.48	0.49	0.49	0.48
1958	0.37	0.37	0.37	0.37	0.37
1959	0.58	0.58	0.58	0.58	0.58
1960	2.47	2.48	2.46	2.42	2.38
1961	11.0	11.0	9.50	8.11	7.10
1962	13.7	13.5	12.9	11.9	11.0
1963	17.2	17.1	16.6	15.7	14.7
1964	20.4	19.9	19.0	18.0	17.1
1965	19.2	19.3	19.3	19.0	18.5
1966	13.4	14.2	15.3	16.4	16.9
$a = 9.4\,E5$	$b = 0.024$	$\rho_0 = 6.3\,E6$			
1956	2.17	2.77	2.71	2.20	1.84
1957	0.54	0.72	1.02	1.24	1.28
1958	0.39	0.40	0.47	0.61	0.72
1959	0.46	0.44	0.45	0.50	0.57
1960	1.03	0.87	0.71	0.64	0.64
1961	2.49	1.68	1.15	0.89	0.82
1962	3.65	2.55	1.67	1.19	1.02
1963	4.77	3.38	2.18	1.50	1.24
1964	5.60	4.07	2.64	1.79	1.45
1965	6.07	4.62	3.07	2.07	1.65
1966	5.62	4.74	3.35	2.30	1.83
1967	2.91	3.25	2.92	2.27	1.88
1968	1.63	1.88	2.01	1.83	1.63
1969	0.98	1.13	1.28	1.29	1.25
1970	0.62	0.72	0.85	0.95	0.98

TABLE 3. Time Dependence of the Atmosphere for Various Model Parameters

Quantities appearing in Table 3 have the following units: $\bar{F}$, 10^{-22} watt/(m^2Hz); $\bar{\rho}_e$, e^-/cm^3; a, e^-/cm^3; b, 10^{22} Hz/watt.

Time, year-quarter		$\bar{F}(t)$	$\bar{\rho}_e(t)$			
			$a = 2.7\,E5$ $b = 0.01$	$a = 8.7\,E5$ $b = 0.01$	$a = 2.7\,E6$ $b = 0.01$	$a = 1.0\,E7$ $b = 0.01$
1956	1	154	4.8 E5	1.5 E6	4.8 E6	1.8 E7
	2	161	5.1 E5	1.6 E6	5.1 E6	1.9 E7
	3	188	6.6 E5	2.1 E6	6.6 E6	2.4 E7
	4	234	1.0 E6	3.3 E6	1.0 E7	3.8 E7
1957	1	202	7.6 E5	2.4 E6	7.6 E7	2.8 E7
	2	220	9.0 E5	2.9 E6	9.0 E6	3.3 E7
	3	228	9.8 E5	3.1 E6	9.8 E6	3.6 E7
	4	277	1.6 E6	5.1 E6	1.6 E7	5.9 E7
1958	1	235	1.0 E6	3.4 E6	1.0 E7	3.9 E7
	2	229	9.9 E5	3.2 E6	9.9 E6	3.6 E7
	3	238	1.1 E6	3.5 E6	1.1 E7	4.0 E7
	4	225	9.5 E5	3.0 E6	9.5 E6	3.5 E7
1959	1	234	1.0 E6	3.3 E6	1.0 E7	3.8 E7
	2	214	8.5 E5	2.7 E6	8.5 E6	3.1 E7
	3	213	8.4 E5	2.7 E6	8.4 E6	3.1 E7
	4	177	5.9 E5	1.9 E6	5.9 E6	2.2 E7
1960	1	170	5.5 E5	1.8 E6	5.5 E6	2.0 E7
	2	164	5.2 E5	1.7 E6	5.2 E6	1.9 E7
	3	169	5.5 E5	1.8 E6	5.5 E6	2.0 E7
	4	143	4.3 E5	1.4 E6	4.3 E6	1.6 E7
1961	1	109	3.3 E5	1.0 E6	3.3 E6	1.2 E7
	2	105	3.2 E5	1.0 E6	3.2 E6	1.2 E7
	3	113	3.4 E5	1.1 E6	3.4 E6	1.2 E7
	4	94	2.9 E5	9.4 E5	2.9 E6	1.1 E7
1962	1	97	3.0 E5	9.6 E5	3.0 E6	1.1 E7
	2	95	3.0 E5	9.5 E5	3.0 E6	1.1 E7
	3	83	2.7 E5	8.8 E5	2.7 E6	1.0 E7
	4	85	2.8 E5	8.9 E5	2.8 E6	1.0 E7
1963	1	78	2.7 E5	8.6 E5	2.7 E6	9.9 E6
	2	83	2.7 E5	8.8 E5	2.7 E6	1.0 E7
	3	81	2.7 E5	8.7 E5	2.7 E6	1.0 E7
	4	81	2.7 E5	8.7 E6	2.7 E6	1.0 E7
1964	1	75	2.6 E5	8.4 E5	2.6 E6	9.7 E6
	2	70	2.6 E5	8.3 E5	2.6 E6	9.5 E6
	3	69	2.6 E5	8.2 E5	2.6 E6	9.5 E6
	4	75	2.6 E5	8.4 E5	2.6 E6	9.7 E6
1965	1	75	2.6 E5	8.4 E5	2.6 E6	9.7 E6
	2	76	2.7 E5	8.5 E5	2.7 E6	9.8 E6
	3	76	2.7 E5	8.5 E5	2.7 E6	9.8 E6
	4	79	2.7 E5	8.6 E5	2.7 E6	9.9 E6
1966	1	87	2.8 E5	9.0 E5	2.8 E6	1.0 E7
	2	97	3.0 E5	9.6 E5	3.0 E6	1.1 E7
	3	110	3.3 E5	1.0 E6	3.3 E6	1.2 E7
	4	116	3.4 E5	1.1 E6	3.4 E6	1.3 E7
1967	1	152	4.7 E5	1.5 E6	4.7 E6	1.7 E7
	2	131	3.9 E5	1.2 E6	3.9 E6	1.4 E7
	3	142	4.3 E5	1.4 E6	4.3 E6	1.6 E7
	4	148	4.5 E5	1.4 E6	4.5 E6	1.7 E7
1968	1	168	5.4 E5	1.7 E6	5.4 E6	2.0 E7
	2	142	4.3 E5	1.4 E6	4.3 E6	1.6 E7
	3	140	4.2 E5	1.3 E6	4.2 E6	1.5 E7
	4	147	4.5 E5	1.4 E6	4.5 E6	1.6 E7
1969	1	160	5.0 E5	1.6 E6	5.0 E6	1.9 E7
	2	154	4.8 E5	1.5 E6	4.8 E6	1.8 E7
	3	139	4.2 E5	1.3 E6	4.2 E6	1.5 E7
	4	151	4.6 E5	1.5 E6	4.6 E6	1.7 E7
1970	1	164	5.2 E5	1.7 E6	5.2 E6	1.9 E7
	2	162	5.1 E5	1.6 E6	5.1 E6	1.9 E7

TABLE 3. (*continued*)

			$\bar{\rho}_e(t)$			
			$a = 2.3\ E5$ $b = 0.02$	$a = 7.4\ E5$ $b = 0.02$	$a = 2.4\ E6$ $b = 0.02$	$a = 7.4\ E6$ $b = 0.02$
1956	1	154	7.1 E5	2.3 E6	7.3 E6	2.3 E7
	2	161	8.1 E5	2.6 E6	8.3 E6	2.6 E7
	3	188	1.4 E6	4.4 E6	1.4 E7	4.4 E7
	4	234	3.4 E6	1.1 E7	3.5 E7	1.1 E8
1957	1	202	1.8 E6	5.7 E6	1.8 E7	5.7 E7
	2	220	2.5 E6	8.2 E6	2.6 E7	8.2 E7
	3	228	3.0 E6	9.6 E6	3.1 E7	9.6 E7
	4	277	7.9 E6	2.5 E7	8.2 E7	2.5 E8
1958	1	235	3.4 E6	1.1 E7	3.5 E7	1.1 E8
	2	229	3.0 E6	9.8 E6	3.1 E7	9.8 E7
	3	238	3.6 E6	1.2 E7	3.7 E7	1.2 E8
	4	225	2.8 E6	9.0 E6	2.9 E7	9.0 E7
1959	1	234	3.4 E6	1.1 E7	3.5 E7	1.1 E8
	2	214	2.3 E6	7.3 E6	2.3 E7	7.3 E7
	3	213	2.2 E6	7.1 E6	2.3 E7	7.1 E7
	4	177	1.1 E6	3.5 E6	1.1 E7	3.5 E7
1960	1	170	9.6 E6	3.1 E6	9.9 E6	3.1 E7
	2	164	8.5 E5	2.7 E6	8.8 E6	2.7 E7
	3	169	9.4 E5	3.0 E6	9.7 E6	3.0 E7
	4	143	5.8 E5	1.9 E6	6.0 E6	1.9 E7
1961	1	109	3.3 E5	1.1 E6	3.4 E6	1.1 E7
	2	105	3.1 E5	1.0 E6	3.2 E6	1.0 E7
	3	113	3.5 E5	1.1 E6	3.6 E6	1.1 E7
	4	94	2.7 E5	8.6 E5	2.8 E6	8.6 E6
1962	1	97	2.8 E5	9.0 E5	2.9 E6	9.0 E6
	2	95	2.7 E5	8.7 E5	2.8 E6	8.7 E6
	3	83	2.4 E5	7.6 E5	2.4 E6	7.6 E6
	4	85	2.4 E5	7.7 E5	2.5 E6	7.7 E6
1963	1	78	2.2 E5	7.2 E5	2.3 E6	7.2 E6
	2	83	2.4 E5	7.6 E5	2.4 E6	7.6 E6
	3	81	2.3 E5	7.4 E5	2.4 E6	7.4 E6
	4	81	2.3 E5	7.4 E5	2.4 E6	7.4 E6
1964	1	75	2.2 E5	7.0 E5	2.2 E6	7.0 E6
	2	70	2.1 E5	6.7 E5	2.1 E6	6.7 E6
	3	69	2.1 E5	6.6 E5	2.1 E6	6.6 E6
	4	75	2.2 E5	7.0 E5	2.2 E6	7.0 E6
1965	1	75	2.2 E5	7.0 E5	2.2 E6	7.0 E6
	2	76	2.2 E5	7.0 E5	2.2 E6	7.0 E6
	3	76	2.2 E5	7.0 E5	2.2 E6	7.0 E6
	4	79	2.3 E5	7.2 E5	2.3 E6	7.2 E6
1966	1	87	2.5 E5	7.9 E5	2.5 E6	7.9 E6
	2	97	2.8 E5	9.0 E5	2.9 E6	9.0 E6
	3	110	3.4 E5	1.1 E6	3.5 E6	1.1 E7
	4	116	3.7 E5	1.2 E6	3.8 E6	1.2 E7
1967	1	152	6.8 E5	2.2 E6	7.0 E6	2.2 E7
	2	131	4.7 E5	1.5 E6	4.8 E6	1.5 E7
	3	142	5.7 E5	1.8 E6	5.9 E6	1.8 E7
	4	148	6.4 E5	2.0 E6	6.5 E6	2.0 E7
1968	1	168	9.2 E5	3.0 E6	9.5 E6	3.0 E7
	2	142	5.7 E5	1.8 E6	5.9 E6	1.8 E7
	3	140	5.5 E5	1.8 E6	5.7 E6	1.8 E7
	4	147	6.2 E5	2.0 E6	6.4 E6	2.0 E7
1969	1	160	7.9 E5	2.5 E6	8.2 E6	2.5 E7
	2	154	7.1 E5	2.3 E6	7.3 E6	2.3 E7
	3	139	5.4 E5	1.7 E6	5.6 E6	1.7 E7
	4	151	6.7 E5	2.2 E6	6.9 E6	2.2 E7
1970	1	164	8.5 E5	2.7 E6	8.8 E6	2.7 E7
	2	162	8.2 E5	2.6 E6	8.5 E6	2.6 E7
1956	1	154	1.1 E6	3.6 E6	1.1 E7	3.5 E7
	2	161	1.4 E6	4.4 E6	1.3 E7	4.2 E7

TABLE 3. (*continued*)

			$\tilde{\rho}_e(t)$			
			$a = 2.1\,E5$ $b = 0.03$	$a = 6.7\,E5$ $b = 0.03$	$a = 2.0\,E6$ $b = 0.03$	$a = 6.4\,E6$ $b = 0.03$
	3	188	3.0 *E*6	9.6 *E*6	2.9 *E*7	9.2 *E*7
	4	234	1.2 *E*7	3.8 *E*7	1.1 *E*8	3.6 *E*8
1957	1	202	4.6 *E*6	1.5 *E*7	4.3 *E*7	1.4 *E*8
	2	220	7.8 *E*6	2.5 *E*7	7.4 *E*7	2.4 *E*8
	3	228	9.9 *E*6	3.1 *E*7	9.4 *E*7	3.0 *E*8
	4	277	4.3 *E*7	1.4 *E*8	4.1 *E*8	1.3 *E*9
1958	1	235	1.2 *E*7	3.9 *E*7	1.2 *E*8	3.7 *E*8
	2	229	1.0 *E*7	3.2 *E*7	9.7 *E*7	3.1 *E*8
	3	238	1.3 *E*7	4.2 *E*7	1.3 *E*8	4.0 *E*8
	4	225	9.0 *E*6	2.9 *E*7	8.6 *E*7	2.7 *E*8
1959	1	234	1.2 *E*7	3.8 *E*7	1.1 *E*8	3.6 *E*8
	2	214	6.5 *E*6	2.1 *E*7	6.2 *E*7	2.0 *E*8
	3	213	6.3 *E*6	2.0 *E*7	6.0 *E*7	1.9 *E*8
	4	177	2.2 *E*6	7.0 *E*6	2.1 *E*7	6.7 *E*7
1960	1	170	1.8 *E*6	5.7 *E*6	1.7 *E*7	5.5 *E*7
	2	164	1.5 *E*6	4.8 *E*6	1.4 *E*7	4.6 *E*7
	3	169	1.7 *E*6	5.6 *E*6	1.7 *E*7	5.3 *E*7
	4	143	8.5 *E*5	2.7 *E*6	8.1 *E*6	2.6 *E*7
1961	1	109	3.6 *E*5	1.2 *E*6	3.5 *E*6	1.1 *E*7
	2	105	3.3 *E*5	1.1 *E*6	3.2 *E*6	1.0 *E*7
	3	113	4.0 *E*5	1.3 *E*6	3.8 *E*6	1.2 *E*7
	4	94	2.7 *E*5	8.5 *E*5	2.5 *E*6	8.1 *E*6
1962	1	97	2.8 *E*5	9.0 *E*5	2.7 *E*6	8.6 *E*6
	2	95	2.7 *E*5	8.6 *E*5	2.6 *E*6	8.3 *E*6
	3	83	2.2 *E*5	7.0 *E*5	2.1 *E*6	6.6 *E*6
	4	85	2.3 *E*5	7.2 *E*5	2.1 *E*6	6.9 *E*6
1963	1	78	2.0 *E*5	6.4 *E*5	1.9 *E*6	6.1 *E*6
	2	83	2.2 *E*5	7.0 *E*5	2.1 *E*6	6.6 *E*6
	3	81	2.1 *E*5	6.7 *E*5	2.0 *E*6	6.4 *E*6
	4	81	2.1 *E*5	6.7 *E*5	2.0 *E*6	6.4 *E*6
1964	1	75	1.9 *E*5	6.1 *E*5	1.8 *E*6	5.9 *E*6
	2	70	1.8 *E*5	5.7 *E*5	1.7 *E*6	5.5 *E*6
	3	69	1.8 *E*5	5.7 *E*5	1.7 *E*6	5.4 *E*6
	4	75	1.9 *E*5	6.1 *E*5	1.8 *E*6	5.9 *E*6
1965	1	75	1.9 *E*5	6.1 *E*5	1.8 *E*6	5.9 *E*6
	2	76	2.0 *E*5	6.2 *E*5	1.9 *E*6	6.0 *E*6
	3	76	2.0 *E*5	6.2 *E*5	1.9 *E*6	6.0 *E*6
	4	79	2.0 *E*5	6.5 *E*5	1.9 *E*6	6.2 *E*6
1966	1	87	2.3 *E*5	7.5 *E*5	2.2 *E*6	7.1 *E*6
	2	97	2.8 *E*5	9.0 *E*5	2.7 *E*6	8.6 *E*6
	3	110	3.7 *E*5	1.2 *E*6	3.5 *E*6	1.1 *E*7
	4	116	4.3 *E*5	1.4 *E*6	4.1 *E*6	1.3 *E*7
1967	1	152	1.1 *E*5	3.5 *E*6	1.0 *E*7	3.3 *E*7
	2	131	6.2 *E*5	2.0 *E*6	5.9 *E*6	1.9 *E*7
	3	142	8.2 *E*5	2.6 *E*6	7.9 *E*6	2.5 *E*7
	4	148	9.7 *E*5	3.1 *E*6	9.2 *E*6	3.0 *E*7
1968	1	168	1.7 *E*6	5.4 *E*6	1.6 *E*7	5.2 *E*7
	2	142	8.2 *E*5	2.6 *E*6	7.9 *E*6	2.5 *E*7
	3	140	7.8 *E*5	2.5 *E*6	7.4 *E*6	2.4 *E*7
	4	147	9.4 *E*5	3.0 *E*6	9.0 *E*6	2.9 *E*7
1969	1	160	1.4 *E*6	4.3 *E*6	1.3 *E*7	4.1 *E*7
	2	154	1.1 *E*6	3.6 *E*6	1.1 *E*7	3.5 *E*7
	3	139	7.6 *E*6	2.4 *E*6	7.3 *E*6	2.3 *E*7
	4	151	1.1 *E*6	3.4 *E*6	1.0 *E*7	3.2 *E*7
1970	1	164	1.5 *E*6	4.8 *E*6	1.4 *E*7	4.6 *E*7
	2	162	1.4 *E*6	4.6 *E*6	1.4 *E*7	4.4 *E*7

TABLE 3. (*continued*)

			$\bar{\rho}_e(t)$	
			$a = 2.0\,E7$ $b = 0.03$	$a = 9.4\,E5$* $b = 0.024$*
1956	1	154	1.1 $E8$	4.3 $E6$
	2	161	1.3 $E8$	4.9 $E6$
	3	188	2.9 $E8$	8.3 $E6$
	4	234	1.1 $E9$	1.8 $E7$
1957	1	202	4.3 $E8$	1.1 $E7$
	2	220	7.4 $E8$	1.4 $E7$
	3	228	9.4 $E8$	1.6 $E7$
	4	277	4.1 $E9$	3.4 $E7$
1958	1	235	1.2 $E9$	1.8 $E7$
	2	229	9.7 $E8$	1.6 $E7$
	3	238	1.3 $E9$	1.9 $E7$
	4	225	8.6 $E8$	1.5 $E7$
1959	1	234	1.1 $E9$	1.8 $E7$
	2	214	6.2 $E8$	1.3 $E7$
	3	213	6.0 $E8$	1.3 $E7$
	4	177	2.1 $E8$	6.7 $E6$
1960	1	170	1.7 $E8$	5.9 $E6$
	2	164	1.4 $E8$	5.2 $E6$
	3	169	1.7 $E8$	5.8 $E6$
	4	143	8.1 $E7$	3.4 $E6$
1961	1	109	3.5 $E7$	1.6 $E6$
	2	105	3.2 $E7$	1.4 $E6$
	3	113	3.8 $E7$	1.7 $E6$
	4	94	2.5 $E7$	1.2 $E6$
1962	1	97	2.7 $E7$	1.2 $E6$
	2	95	2.6 $E7$	1.2 $E6$
	3	83	2.1 $E7$	9.7 $E5$
	4	85	2.1 $E7$	1.0 $E6$
1963	1	78	1.9 $E7$	8.9 $E5$
	2	83	2.1 $E7$	9 7 $E5$
	3	81	1.9 $E7$	9.4 $E5$
	4	81	2.1 $E7$	9.4 $E5$
1964	1	75	2.0 $E7$	8.4 $E5$
	2	70	2.0 $E7$	7.8 $E5$
	3	69	1.8 $E7$	7.7 $E5$
	4	75	1.7 $E7$	8.4 $E5$
1965	1	75	1.7 $E7$	8.4 $E5$
	2	76	1.9 $E7$	8.6 $E5$
	3	76	1.9 $E7$	8.6 $E5$
	4	79	1.9 $E7$	9.1 $E5$
1966	1	87	2.2 $E7$	1.0 $E6$
	2	97	2.7 $E7$†	1.2 $E6$
	3	110	2.4 $E7$†	1.6 $E6$
	4	116	5.2 $E7$†	1.8 $E6$
1967	1	152		4.2 $E6$
	2	131		2.6 $E6$
	3	142		3.3 $E6$
	4	148		3.9 $E6$
1968	1	168		5.6 $E6$
	2	142		3.3 $E6$
	3	140		3.2 $E6$
	4	147		3.8 $E6$
1969	1	160		4.8 $E6$
	2	154		4.3 $E6$
	3	139		3.1 $E6$
	4	151		4.1 $E6$
1970	1	164		5.2 $E6$
	2	162		5.0 $E6$

* Calculated by using the values $\rho_e(S = 70) = 3.2\,E5$, $\rho_e(S = 100) = 9.4\,E5$, $\rho_e(S = 150) = 3.80\,E6$, $\rho_e(S = 200) = 1.05\,E7$, and $\rho_e(S = 250) = 2.24\,E7$, and fits of the form given in (81) at points in between.
† Calculated by using $\bar{F}$ values of 98, 92, and 126 for the times 1966-2, 3, and 4, respectively.

to examine the conjectured inequality

$$S > \text{nt}? \qquad (B10)$$

which, by using equations 4, 36, 41, and $B9$, can be recast in the form

$$\chi j_n^{\sigma a}/(\gamma v t_n) > \sigma_0(E)(1/7)[\overline{\rho_e \mathcal{J}}(>E)]? \qquad (B11)$$

We will calculate numerical values for both sides of (B11). We consider, for example, the case where $E = 55$ Mev. (Only low energies are of interest, since it is only there that the reaction (B1) is expected to make a noticeable contribution.) The right-hand side of (B11) can be conveniently estimated from the data of *Filz and Holeman* [1965]. We first compute the average of ρ_e (at fixed B and L) over all longitudes and denote the result by $<\rho_e>_{\text{long ave}}$.

Then, by using the data of Filz and Holeman and the spectral shape of Figure 1, we find

$$[\mathcal{J}(E > 55)\langle\rho_e\rangle_{\text{long ave}}]\Big|_{\substack{B=0.23\\L=1.4}} \simeq 10^{10}\ \text{cm}^{-5}\ \text{sec}^{-1} \qquad (B12)$$

The values of B and L employed in (B12) correspond to a mirror altitude of 310 km in the south Atlantic magnetic anomaly. In computing $\langle\rho_e\rangle$, we used the Harris-Priester atmosphere for $S = 150$ and the 48-term magnetic field expansion. The measurements of Filz and Holeman were made in 1961 to 1962 when $S \sim 100$. We used a somewhat larger value of S to take into account the fact that what we really want is a 'solar cycle averaged' result. We next observe that the product $[\mathcal{J}(E > 55)\langle\rho_e\rangle]$ is approximately constant along a field line in the southern hemisphere. (It is in fact a slightly decreasing function for decreasing B.) Of course, in the northern hemisphere the product is much smaller since the minimum mirror points there are much higher. Thus, to good approximation,

$$(\overline{\rho_e \mathcal{J}}) \simeq 5 \times 10^9 \text{ cm}^{-5} \text{ sec}^{-1} \qquad (B13)$$

A σ_0 obeying ($B8$) at 55 Mev can be inferred from the work of Corley, Wall, and Roos who studied reaction ($B1$) for carbon. From the data of *Wall and Roos,* [1966], we find that a satisfactory value of $\sigma_0(E)$ for $E = 55$ Mev and $E' = 160$ Mev is $\sim$0.2 mb/(Mev ster). The data of *Corley* (1968) at $E' = 1$ bev also satisfy ($B8$) for $\sigma_0(E)$ $\sim$0.2 mb/(Mev ster) and E in the range 700–800 Mev. Unfortunately his data do not extend to lower values of E although, within the range $E \sim 750$ Mev, σ_0 is a decreasing function of energy. The data at both $E' = 160$ Mev and 1 bev indicate that reaction ($B1$) takes place almost entirely with the production of a single proton (i.e., $n = 2$) for the values of E considered. Since only values of $E \sim 750$ Mev have been measured at $E' = 1$ bev, we cannot be sure (and even suspect the contrary) that single proton production will still dominate at $E \sim 55$ Mev. Thus, as a cautious estimate, we use the value

$$\sigma_0 \sim 8 \times 0.2 = 1.6 \text{ mb/(ster Mev)} \qquad (B14)$$

in the remainder of our calculations. This higher value takes into account the possibility that atmospheric nuclei may be completely broken up (for $E' \gg E$) with essentially the same cross section per nucleon as single proton production.

It is now an easy matter to estimate the right-hand side of ($B11$). Upon combining terms, we find

$$\sigma_0(1/7)(\overline{\rho_e \mathcal{J}}) \sim 10^{-18} \text{ (cm}^3 \text{ sec Mev)}^{-1} \quad (B15)$$

To compute the left-hand side of ($B11$), we use (42) multiplied by a factor of 50 and set $\chi \sim (1/10)$. One finds, for $E = 55$ Mev,

$$\chi j_n^{\,ea}/(\gamma v t_n) \sim 10^{-17} \text{ (cm}^3 \text{ sec Mev)}^{-1} \qquad (B16)$$

We now see that the inequality ($B11$) is well satisfied, and we conclude that our neglect of the process ($B1$) produces at most a 10% error.

We next turn to the effect of the higher order terms in the Taylor series of equation 16. In neglecting them, we neglected the fact that nuclear Coulomb scattering is not entirely in the forward direction, and that multiple Coulomb scattering tends to produce diffusion in pitch angle. We will see that this effect is small, but not uninteresting.

In traversing a distance dx in a medium, a charged particle undergoes a mean square angular deflection given approximately by the relation

$$d\langle\theta^2\rangle = [21/(pv)]^2 X_{\text{rad}}^{-1}\, dx \qquad (B17)$$

where (pv) is given in Mev and X_{rad} is the radiation length of the medium [*Ritson,* 1961]. Thus, for example, in slowing down from an energy of 500 to 30 Mev, a proton is expected to experience a mean square deflection given by

$$\langle\theta^2\rangle = (21)^2 X_{\text{rad}}^{-1} \int_{30}^{500} (pv)^{-2}(-dx/dE)\, dE \qquad (B18)$$

For air, $X_{\text{rad}} = 37$ g/cm². By using the values of dE/dx given by *Rich and Madey* [1954] and by evaluating the integral in ($B18$) numerically, we find

$$\langle\theta^2\rangle^{1/2} \sim 7° \qquad (B19)$$

We conclude that diffusion in pitch angle due to multiple scattering is relatively small. This conclusion becomes stronger for higher energy particles because of the $(pv)^{-2}$ term in the integrand. We should also point out that ($B19$) represents an overestimate, since not all 30-Mev protons arise from the slowing down of 500-Mev protons. Many come from the slowing down of lower energy protons.

Although diffusion in pitch angle due to multiple scattering is small, its effect is not entirely negligible at low altitudes where even a slight change in pitch angle produces a rather large change in the average atmospheric density experienced by a particle. If a particle with local pitch angle α_l scatters through an angle $\Delta\alpha_l$, its mirror point magnetic field changes by an amount

$$\Delta B_m/B_m = -2\, \Delta\alpha_l \cot \alpha_l \qquad (B20)$$

From Figure 8 we see that for $L = 1.4$ and $B_m = 0.21$ a 5% change in B_m produces a factor of 5 change in the trajectory averaged atmospheric density. Of course, most pitch angle scattering will occur near the mirror point where the atmospheric density is largest. If we imagine that all scatterings in our example ($B_m = 0.21$) take place in a region where the atmospheric density is greater or equal to ⅓ of the mirror density, we find

$$\cot \alpha_l \simeq 0.2 \tag{B21}$$

Inserting this result into (B20) and using the estimate, (B19) gives $\Delta B_m/B_m \sim 5\%$. Thus, in making a detailed theoretical prediction of the spatial dependence of fluxes at low altitudes, one should include diffusion in pitch angle due to multiple scatterings.

Acknowledgments. This work was begun at Aerospace Corporation. Much of the numerical work was performed at the Computer Science Center of the University of Maryland. Computer and drafting charges were financed through NASA grant NGR 21-002-002. This work was supported in part by the United States Air Force under grant AFOSR 68-1453.

* * *

The Editor wishes to thank T. A. Farley and another referee for their assistance in evaluating this paper.

REFERENCES

Barkas, W. H., and S. Van Friesen, High-velocity range and energy-loss measurements in Al, Cu, Pb, U, and emulsion, *Nuov. Cim. Suppl., 19,* 41. 1961.

Birmingham, T. J., Convection electric fields and the diffusion of trapped magnetospheric radiation, *J. Geophys. Res., 74,* 2169, 1969.

Birmingham, T. J., T. G. Northrop, and C. -G. Fälthammer, Charged particle diffusion by violation of the third adiabatic invariant, *Phys. Fluids, 10,* 2389, 1967.

Blanchard, R. C., and W. N. Hess, Solar cycle changes in inner-zone protons, *J. Geophys. Res., 69,* 3927, 1964.

Bourdeau, R. E., S. Chandra, and W. M. Neupert, Time correlation of extreme ultraviolet radiation and thermospheric temperature, *J. Geophys. Res., 69,* 4531, 1964.

Chen, F. F., C. P. Leavitt, and A. M. Shapiro, Attenuation cross sections for 860-Mev protons, *Phys. Rev., 99,* 857, 1955.

Conrath, B. J., Radial diffusion of trapped particles with arbitrary pitch angle, *J. Geophys. Res., 72,* 6069, 1967.

Corley, D. M., Quasi-free scattering of 1 Gev protons from C^{12} and Ca^{40}, Ph.D. thesis, University of Maryland, College Park, 1968.

Cornwall, J. M., A. R. Sims, and R. S. White, Atmospheric density experienced by radiation belt protons, *J. Geophys. Res., 70,* 3099, 1965.

DeForest, S. E., Long term variations in high-energy geomagnetically trapped particles, Ph.D. thesis, University of California, San Diego. 1970.

Dragt, A. J., Effect of hydromagnetic waves on the lifetime of Van Allen radiation protons, *J. Geophys. Res., 66,* 1641–1649, 1961.

Dragt, A. J., M. M. Austin, and R. S. White, Cosmic ray and solar proton albedo neutron decay injection, *J. Geophys. Res., 71,* 1293, 1966.

Environmental Science Services Administration, *Solar Geophysical Data,* U.S. Dep. of Commerce, Washington, D. C., 1961 through 1968.

Fälthammer, C. -G., Radial diffusion by violation of the third adiabatic invariant, in *Earth's Particles and Fields,* edited by B. M. McCormac, p. 157, Reinhold. New York, 1968.

Farley, T. A., A. D. Tomassian, and M. C. Chapman, Evaluation of the Crand source for 10- to 50-Mev trapped protons, *J. Geophys. Res., 74,* 4721, 1969.

Fenton, K. B., A search for α particles trapped in the geomagnetic field, *J. Geophys. Res., 72,* 3889, 1967.

Filz, R. C., and E. Holeman, Time and altitude dependence of 55-Mev trapped protons, August 1961 to June 1964, *J. Geophys. Res., 70,* 5807–5822, 1965.

Freden, S. C., and R. S. White, Trapped protons and cosmic ray albedo neutron fluxes, *J. Geophys. Res., 67,* 25. 1962.

Harris, I., and W. Priester, Time-dependent structure of the upper atmosphere, *NASA TND-1443,* Goddard Space Flight Center, Greenbelt, Md., 1962*a*.

Harris, I., and W. Preister, Theoretical models for the solar-cycle variation of the upper atmosphere, *NASA TND-1444,* Goddard Space Flight Center, Greenbelt, Md., 1962*b*.

Harris, I., and W. Priester, Relation between theoretical and observational models of the upper atmosphere, *NASA X-640-63-145,* Goddard Space Flight Center, Greenbelt, Maryland, 1963.

Haymes, R. C., Fast neutrons in the earth's atmosphere, *J. Geophys. Res., 69,* 841, 1964.

Heckman, H. H., and V. O. Brady, Effective atmospheric losses for 125 Mev protons in south Atlantic anomaly, *J. Geophys. Res., 71,* 2791, 1966.

Hendricks, S. J., and J. C. Cain, Magnetic field data for trapped particle evaluations, *J. Geophys. Res., 71,* 346, 1966.

Hess, W. N., Van Allen belt protons from cosmic ray neutron leakage, *Phys. Rev. Lett., 3,* 11, 1959.

Holt, S. S., R. B. Mendell, and S. A. Korff, Fast neutron variations in the atmosphere at solar minimum, *J. Geophys. Res., 71,* 5109, 1966.

Hughes, D. J., and R. B. Schwartz, Neutron cross sections, *Brookhaven National Lab. Rep. BNL 325,* second edition, 1958.

Intriligator, D. S., Albedo neutron source for high-energy protons trapped in the geomagnetic field, *Phys. Rev. Lett., 20,* 1048 and 1333, 1968.

Jensen, D. C., and W. A. Whitaker, A spherical harmonic analysis of the geomagnetic field, *J. Geophys. Res., 65,* 2500, 1960.

Jensen, D. C., and J. C. Cain, An interim geomagnetic field, *J. Geophys. Res., 67,* 3568, 1962.

Johnson, F. S., Atmospheric structure, *Astronaut. Aeronaut., 7,* 54, 1962.

Kellogg, P. J., Van Allen radiation of solar origin, *Nature, 183,* 1295, 1959.

King, J. H., Models of the trapped radiation environment, vol. 4, Low energy protons, *NASA SP-3024,* Goddard Space Flight Center, Greenbelt, Md., 1967.

Krimigis, S. M., and J. A. Van Allen, Geomagnetically trapped alpha particles, *J. Geophys. Res., 72,* 5779, 1967.

Kuiper, G. P., editor, *The Sun,* University of Chicago Press, Chicago, Ill., 1953.

Lenchek, A. M., and S. F. Singer, Geomagnetically trapped protons from cosmic ray albedo neutrons, *J. Geophys. Res., 67,* 1263–1287, 1962.

Lindstrom, P. J., and H. H. Heckman, *B–L* space and geomagnetic field models, *J. Geophys. Res., 73,* 3441, 1968.

Lingenfelter, R. E., The cosmic ray neutron leakage flux, *J. Geophys. Res., 68,* 5633, 1963.

Mather, R., and E. Segre, Range Energy relation for 340-Mev protons, *Phys. Rev., 84,* 191, 1951.

Nakada, M. P., and G. D. Mead, Diffusion of protons in the outer belt, *J. Geophys. Res., 70,* 4777, 1965.

Nakada, M. P., J. W. Dungey, and W. N. Hess, On the origin of outer-belt protons, *J. Geophys. Res., 70,* 3529, 1965.

Neupert, W. M., Intensity variations in the solar extreme ultraviolet spectrum observed by Oso 1, *Astronomical observations from space vehicles,* edited by J. -L. Steinberg, *Ann. Astrophys., 28,* 446, 1965.

Neupert, W. M., The solar corona above active regions: A comparison of extreme ultraviolet line emission with radio emission, *Solar Phys., 2,* 294. 1967.

Rich, M., and R. Madey, Range-energy tables, *Univ. Calif. Radiation Lab. Rep. UCRL-2301,* 1954.

Ritson, D. M., *Techniques of High Energy Physics,* Interscience, New York, 1961.

Roos, P. G., Elastic and inelastic scattering of high energy protons from nuclei, Ph.D. thesis, Massachusetts Institute of Technology, Boston, Mass., 1964.

Singer, S. F., Trapped albedo theory of the radiation belt, *Phys. Rev. Lett., 1,* 181, 1958.

Vette, J. I., Models of the trapped radiation environment, vol. 1: Inner zone protons and electrons, *NASA SP-3024,* Goddard Space Flight Center, Greenbelt, Md., 1966.

Wall, N. S., and P. R. Roos, Quasi-free scattering of 160-Mev protons from nuclei, *Phys. Rev., 150,* 811, 1966.

(Received July 28, 1970;
revised October 15, 1970.)